1-1-2014

Microtubule Dynamics, Kinetochore Number, and Kinetochore Distribution in Cells Undergoing Mitosis with Unreplicated Genomes

Manuella Rossette Clarkotton

Microtubule dynamics, kinetochore number, and kinetochore distribution in cells undergoing mitosis with unreplicated genomes

By

Manuella Rossette Clark-Cotton

A Thesis
Submitted to the Faculty of
Mississippi State University
in Partial Fulfillment of the Requirements
for the Degree of Master of Science
in Biological Sciences
in the Department of Biological Sciences

Mississippi State, Mississippi

May 2014

Microtubule dynamics, kinetochore number, and kinetochore distribution in cells undergoing mitosis with unreplicated genomes

By

Manuella Rossette Clark-Cotton

Approved:

_____

Dwayne A. Wise
(Major Professor)

_____

Daniel G. Peterson
(Minor Professor and Committee Member)

_____

Donna M. Gordon
(Committee Member)

_____

Gary N. Ervin
(Committee Member)

_____

R. Gregory Dunaway
Professor and Dean
College of Arts & Sciences

Name: Manuella Rossette Clark-Cotton

Date of Degree: May 17, 2014

Institution: Mississippi State University

Major Field: Biological Sciences

Major Professor: Dr. Dwayne A. Wise

Title of Study: Microtubule dynamics, kinetochore number, and kinetochore distribution in cells undergoing mitosis with unreplicated genomes

Pages in Study: 62

Candidate for Degree of Master of Science

In cells undergoing mitosis with unreplicated genomes (MUG), anaphase is successfully initiated despite the abundance of kinetochores that are attached to microtubules emanating from both spindle poles (merotely). In cultured cells, merotely is associated with lagging at the metaphase plate. Treatment with microtubule-perturbing drugs alters the frequency of lagging, but the effect of these drugs on MUG cells is unclear. In this study, low doses of a microtubule-stabilizing drug, taxol, or a microtubule-destabilizing drug, nocodazole, dramatically increased the frequency of lagging kinetochores in the midbody of MUG daughter cell pairs. Likewise, increasing the kinetochore number increased the frequency of lagging kinetochores. In this thesis, these data are used to propose a model of mitosis in which the bipolar attachments of MUG cells are reduced to monopolar attachments that are stabilized by their perpendicular orientation with respect to the kinetochore, allowing for spindle assembly checkpoint satisfaction without centromeric tension.

Key words: mitosis, MUG cells, kinetochores, merotely

DEDICATION

This thesis is dedicated to my parents, Manuel and AlPaulthenia Cotton, and to the memory of my grandmother, Pauline McReynolds Clark.

ACKNOWLEDGEMENTS

The author gratefully acknowledges the assistance of her major professor, Dr. Dwayne A. Wise, for his patience and generosity; members of her thesis committee, Dr. Donna M. Gordon and Dr. Daniel G. Peterson, for critical reviews of the research project and previous drafts of the thesis; Ms. Amanda Lawrence of the Mississippi State University Institute for Imaging and Analytical Technologies, for technical assistance with confocal microscopy; and Dr. Janice DuBien, for guidance with statistical analyses.

TABLE OF CONTENTS

LIST OF TABLES

LIST OF FIGURES

CHAPTER I

INTRODUCTION

Mitosis and the Eukaryotic Cell Cycle

Mitosis has been described cytogenetically since the 19th century (Flemming, 1882). Although it is a process common to all eukaryotes, its details vary considerably from yeasts (Biggins, 2013) to vertebrates (Foley and Kapoor, 2013) with regard to the breakdown of the nuclear envelope, the structure of the kinetochore, and the attachment of chromosomes to the mitotic spindle.

In a typical vertebrate cell, mitosis is composed of five cytological substages: prophase, prometaphase, metaphase, anaphase, and telophase. In prophase, the chromosomes begin to condense into chromatin that is visible by light microscopy, the duplicated centrosomes migrate around the nuclear envelope to opposite sides of the cell, and the microtubules are organized into a mitotic spindle, the poles of which emanate from the centrosomes. Prometaphase is characterized by the disassembly of the nuclear envelope and the attachment of chromosomes to the spindle. At metaphase, the chromosomes are aligned at the equator of the spindle, known as the metaphase plate. Anaphase begins when the sister chromatids separate, moving to opposite spindle poles by two distinct mechanisms. In anaphase A, the spindle microtubules shorten without movement of the poles, and in anaphase B, the poles themselves move further apart. Finally, in telophase, the nucleus returns to its pre-mitotic state: the spindle is

disassembled; the chromosomes decondense; and nuclear envelopes reassemble around the chromosomes, forming two nuclei. Telophase is usually accompanied or followed by cytokinesis, the division of the cytoplasm into two cells, each with a single nucleus (Morgan, 2007).

A molecular understanding of mitosis began to develop with a description of the complete cell cycle, including the non-mitotic stages, in cells cultured from a variety of species. By the 1950s, researchers had observed that DNA was replicated during late interphase (Deeley et al., 1954), and by the 1960s, it was known that cells in interphase and mitosis responded differently to ultraviolet (Swann, 1962), gamma (Hsu et al., 1962), and x-ray irradiation (Monesi, 1962). Throughout much of this decade, three stages were commonly described: G1, from the initiation of mitosis to the beginning of replication; S, during which replication occurred; and G2, extending from post-replication until the next mitosis (Sisken and Kinosita, 1961). By the late 1960s, scientists knew that the pre-mitotic and mitotic stages were biochemically distinct, both in terms of catabolism (Van't Hof, 1968) and anabolism (Martin et al., 1969), and the designations G1 (pre-replication), S (replication), G2 (pre-mitosis), and M (mitosis and cytokinesis) became standard. Once these stages were defined, experiments with fused cells demonstrated that factors present in cells at different stages exerted control over the cycle: a G1-S fusion caused replication in the G1 cell, while a S-G2 fusion delayed the G2 cell's entry into M (Johnson and Rao, 1970; Rao and Johnson, 1970).

Genetic studies of *Saccharomyces cerevisiae* mutants led to the identification of the *Cdc* genes controlling the cell cycle (Hartwell et al., 1974; Hartwell et al., 1970). This work was extended in the *Xenopus laevis* embryo with the discovery of **m**aturation-

promoting **f**actor (MPF), later shown to be a complex of two cell cycle regulatory proteins (Masui and Markert, 1971). These proteins were characterized as belonging to two classes: cyclins and **c**yclin-**d**ependent **k**inases (Cdks). Researchers have identified three groups of cyclins, each abundant at a characteristic point in the cell cycle: G1/S cyclins, peaking in late G1 and governing the transition into S phase; S cyclins, rising in late G1 and remaining at a high concentration until M; and M cyclins, reaching a maximum concentration at entry into M and remaining elevated until the initiation of anaphase. (A fourth class, the G1 cyclins, regulates the cell's response to extracellular factors.) Each cyclin binds to and activates a class of Cdks, whose levels are constant throughout the cell cycle. Therefore, the level of cyclin at a given point in the cycle determines the activity of its partner Cdk. As regulatory kinases, Cdks phosphorylate the molecules that initiate transitions in the cell cycle. For example, the M cyclin-Cdk complex causes events that lead to the breakdown of the nuclear envelope, the migration of the centrosomes to opposite poles, and the formation of the mitotic spindle (Morgan, 1997). Additional levels of regulation are provided by inhibitors (including the phosphatase Cdc25, the kinase Wee1, and **C**d**k** **i**nhibitory binding proteins, or CKIs), activators (**C**dk-**a**ctivating **k**inases, or CAKs), and mechanisms that control the rate of protein degradation and synthesis (Morgan, 2007).

Cell Cycle Checkpoints

The genetic data used to develop the notion of a cell cycle also suggested the existence of discrete checkpoints that both respond to and influence (through feedback mechanisms) the levels of cyclins, controlling the progression of the cell cycle (Leland and Weinert, 1989). Three checkpoints have been well-described: the G1/S checkpoint,

or Start, which controls entry into S phase; the G2/M checkpoint, or DNA damage checkpoint, which monitors entry into M phase; and the metaphase-to-anaphase transition, or spindle assembly checkpoint, which controls the initiation of anaphase. When the regulatory molecules of each checkpoint are properly activated, that checkpoint is said to be satisfied, and the transition to the next stage of the cell cycle occurs. A satisfied checkpoint is said to be "off," while an unsatisfied checkpoint is considered "on." The G1/S checkpoint responds to extracellular proliferation factors (i.e., mitogens) that signal the need for cell division (Morgan, 2007).

The DNA damage checkpoint prevents the initiation of M phase when DNA is damaged or incompletely replicated. The kinases ATM (**a**taxia **t**elangiectasia **m**utated) and ATR (**a**taxia **t**elangiectasia mutated and **R**ad-3-related) are essential to DNA damage recognition (Jackson, 1996), ATM for double-strand breaks and ATR for single-stranded DNA. The recruitment of either ATM or ATR to damaged DNA causes the activation of Chk2 or Chk1 (Matsuoka et al., 1998), kinases that phosphorylate cell cycle proteins to temporarily prevent the initiation of mitosis. In metazoans, this pathway activates the well-known tumor suppressor p53 to prevent the proliferation of cells with damaged DNA by causing an irreversible arrest (Morgan, 2007). Caffeine is a well-established inhibitor of ATM and ATR (Sarkaria et al., 1999).

The spindle assembly checkpoint (SAC) controls the transition from metaphase to anaphase by regulating the activity of the **a**naphase-**p**romoting **c**omplex/**c**yclosome (APC/C), a ubiquitin ligase. As noted above, M cyclin levels are high as mitosis begins. These levels remain elevated until the satisfaction of the SAC, which coincides with the alignment of chromosomes at the metaphase plate, although exactly which conditions are

required to turn the SAC off is still debated (see *Spindle Assembly Checkpoint Satisfaction* below). Activation of the APC/C depends on the binding of the cofactor Cdc20, a constituent of the **m**itotic **c**heckpoint **c**omplex (MCC). When the MCC is disassembled, Cdc20 binds and activates the APC/C, which ubiquitinates M cyclins, leading to their destruction by the proteasome and the inactivation of M cyclin-Cdk complexes. The APC/C also ubiquitinates the regulatory molecule securin, which binds the protease separase. When released from securin, separase cleaves cohesin, the molecule that binds sister chromatids together from S phase through metaphase, allowing the chromatids to move to different poles (Musacchio and Salmon, 2007). Despite its name, the SAC does not simply monitor the organization of the mitotic spindle, but rather it reports the status of spindle-chromosome interactions. The precise nature of the interactions that satisfy the SAC remains under intense investigation, but most researchers describe these requirements in terms of chromosome attachment to the mitotic spindle and/or tension across the attached chromosome (Pinsky and Biggins, 2005).

The Mitotic Spindle and Microtubule Dynamics

The mitotic spindle is a dynamic assembly of microtubules and associated proteins. Microtubules are polymerized from tubulin α/β heterodimers (Inoué and Sato, 1967; Kiefer et al., 1966) to produce a minus end that emanates from the microtubule-organizing center (the centrosome in animal cells) and a plus end that interacts with the kinetochore, which is described below (Bergen et al., 1980). Microtubules grow and shrink at both ends, although both processes occur more quickly at the plus end. Both subunits of the dimer bind a molecule of GTP, but only the β subunit has GTPase

activity. When capped by a GTP-bound tubulin dimer at the plus end, microtubules grow, but the loss of this cap causes shrinkage at the plus end. The tendency to rapidly shift between growth and shrinkage, called *catastrophe*, or from shrinkage to growth, known as *rescue*, is called *dynamic instability*. Mitotic microtubules exhibit markedly greater dynamic instability than interphase microtubules, a feature that is believed to contribute to kinetochore capture (Morgan, 2007).

The Kinetochore

The attachment of a chromosome to the mitotic spindle is mediated by a structure called the *kinetochore*, an assembly of structural and regulatory proteins found at the centromere of each chromosome. Although the structure of kinetochores and their interactions with microtubules vary greatly among species (McIntosh et al., 2013), the following description is limited to the mammalian kinetochore and its proteins. Fluorescence microscopy reveals that kinetochores are assembled shortly after DNA replication (Brenner et al., 1981). The trilaminar structure of a mammalian kinetochore can be observed with electron microscopy, with an inner kinetochore that binds the centromere, a middle layer, and an outer kinetochore that binds microtubules (Brinkley and Stubblefield, 1966; Jokelainen, 1967). When microtubules are not bound, a fibrous corona occupies the microtubule-binding region (Cheeseman and Desai, 2008).

The organization of kinetochore proteins is complex and changes in predictable ways throughout the cell cycle. Those described below are those that form the constitutive kinetochore structure, and those that are most important for microtubule attachment, error correction, SAC satisfaction, and anaphase initiation.

Two groups of centromere proteins are generally considered part of the kinetochore. **Cen**tromere **p**rotein **A** (CENP-A, a variant of histone H3), CENP-B, CENP-C, and others are found at the centromere from S phase through mitosis and form the **c**onstitutive **c**entromere-**a**ssociated **n**etwork (CCAN). A second centromere protein network, the chromosomal passenger complex (CPC), consists of **in**ner **cen**tromere **p**rotein (INCENP), Survivin, Borealin, and Aurora B kinase, and mediates the correction of kinetochore-microtubule attachment errors. The **m**itotic **c**entromere-**a**ssociated **k**inesin (MCAK) has also been localized to the centromere, near the CPC (Musacchio and Salmon, 2007). One unresolved question involves how Aurora B, which is found at the centromere through metaphase, could facilitate the correction of errors at the outer kinetochore, where the microtubules attach. As anaphase begins, Aurora B relocates to the spindle midzone, and then to the midbody of the cell in telophase/cytokinesis (Varma and Salmon, 2012).

Three proteins complexes found at the outer kinetochore form the microtubule binding sites: **K**NL-1, the **M**IS12 complex, and the **N**dc80 complex, collectively called the KMN network (Cheeseman et al., 2006; Cheeseman et al., 2004). The precise arrangement of these proteins is beyond the scope of this review, but they clearly must allow for both stable attachments (that are secure from prometaphase through anaphase) and dynamic microtubules (to allow for the development of a spindle, the capture and binding of kinetochores, and the depolymerization of microtubules in anaphase).

In yeast, the Dam1 complex is believed to form a ring that surrounds the plus end of a microtubule, while coiled-coils (including the Ndc80 complex) extend from the ring to the inner kinetochore, tethering the microtubule and kinetochore to each other. In this

way, the microtubule is stably connected to the kinetochore but is still able to gain and lose subunits from its plus end. However, Dam1 has not been observed in metazoans, so their kinetochore-microtubule binding strategy is unknown (Morgan, 2007). Components of the KMN network and Dam1 are known substrates of Aurora B kinase (Liu and Lampson, 2009), although given their different locations in the mitotic cell, the functional significance of this finding is unknown. **P**olo-**l**ike **k**inase **1** (Plk1) is also found at the outer kinetochore. Its substrate, 3F3/2, appears in phosphorylated form in the absence of tension but is cleared from kinetochores when tension is present (Pinsky and Biggins, 2005).

In the corona region are the classic SAC proteins, including BubR1, Bub3, and Mad2. Mad2 is a microtubule-kinetochore detachment marker that begins mitosis on the kinetochore but relocates when kinetochores bind to the spindle (Musacchio and Salmon, 2007). Treatments that disrupt the attachments (i.e., nocodazole) will cause Mad2 to return to the kinetochore (Waters et al., 1998). When all kinetochores are stably bound to microtubules and anaphase begins, Mad2 relocates to the spindle midzone. Also found in the corona region are Cdc20 and the APC/C (Musacchio and Salmon, 2007). As discussed previously, Cdc20 is the cofactor required to activate the APC/C, the ubiquitin ligase whose activity leads to the destruction of the mitotic cyclins. Notably, both Cdc20 and Mad2 exist in soluble and bound forms (Cheeseman and Desai, 2008).

Kinetochore-Microtubule Attachment and Correction

Kinetochores attach to the spindle in prometaphase and can be either mono-oriented (with the chromosome linked to only one spindle pole) or bi-oriented (the chromosome linked to both poles) (Pinsky and Biggins, 2005). Mono-orientation can be

either monotelic (only one kinetochore is attached to one pole) or syntelic (both kinetochores are attached to a single pole). While monotely is a normal stage of attachment, syntely requires correction. Specifically, syntelic attachments signal the SAC to delay anaphase until they are corrected (Musacchio and Salmon, 2007). Bi-orientation can be either amphitelic or merotelic. Amphitelic attachments, defined as each sister kinetochore linked to one pole, are normal. Merotelic attachments occur when both kinetochores are amphitelically linked but one kinetochore has one or more additional attachments to the opposite pole. Merotelic attachments are not thought to be recognized by the SAC, and anaphase can be initiated without their correction (Cimini et al., 2001). Experiments have demonstrated that merotely is a major mechanism for aneuploidy, the transmission of an abnormal number of chromosomes, in mitosis (Cimini et al., 2001; Cimini et al., 2003).

The process of attachment was first described in four stages: 1) One kinetochore of a replicated chromosome is captured by a single microtubule, forming a monotelic, mono-oriented attachment to the lateral surface of a single microtubule; 2) the captured chromosome moves poleward; 3) the attachment is converted to an end-on, or perpendicular, attachment as more microtubules bind the still mono-oriented chromosome; and 4) the capture of the sister kinetochore by microtubules from the opposite pole produces a bi-oriented chromosome (Rieder and Alexander, 1990). More recently, studies have shown that the steps between initial capture and bi-orientation involve a number of reorientations and corrections (Tanaka et al., 2005).

Although kinetochore-microtubule attachments are sometimes described as intrinsically stable or unstable (Morgan, 2007), data have clearly demonstrated that

specific molecules are required to efficiently correct attachment errors. The protein most commonly invoked as the facilitator of kinetochore-microtubule error corrections is Aurora B kinase. Whether it senses the absence of tension, an abnormal geometrical arrangement, or some other factor is unknown, but its importance is unquestionable. Aurora B was first identified as a mediator of syntelic error correction (Hauf et al., 2003) and was later shown to facilitate the correction of merotelic errors, which are not identified by the SAC, and therefore, can be maintained into anaphase (Cimini, 2007).

Three molecules have been identified as key substrates of Aurora B kinase in the context of its error correction role: the Dam1 complex, the Ndc80 complex (called Hec1 in humans), and the mitotic kinesin MCAK. Dam1 (not found in metazoans) forms a ring around the microtubule near its plus end. It is not required for the initial capture of kinetochores but has been implicated in the achievement of bi-orientation (Tanaka et al., 2005). The other two molecules are believed to regulate microtubule dynamics. It is not obvious that microtubule dynamics would be important in error correction, since the Dam1-Ndc80 complex model of a kinetochore tethered to the microtubule's plus end predicts that the plus end remains free to polymerize and depolymerize (Morgan, 2007). Nevertheless, the absence of Hec1 leads to the loss of microtubule dynamics at the plus end and the inability to detach kinetochores (DeLuca et al., 2006), and the loss of MCAK renders kinetochore microtubules unable to depolymerize (Knowlton et al., 2006). In the absence of both Hec1 and MCAK, the rates of error correction drop. Therefore, normal microtubule dynamics are thought to be required for error correction.

Spindle Assembly Checkpoint Satisfaction

As previously noted, certain kinetochore-microtubule attachment errors, such as syntely, are recognized by the SAC, while others, like merotely, are not, although both types of error are corrected by Aurora B kinase (Musacchio and Salmon, 2007). Monotely (the attachment of only one sister kinetochore to the spindle) clearly produces SAC activation, which can be demonstrated by the presence of Mad2 at unattached kinetochores (Waters et al., 1998). Others have argued that tension is required. When tension is lacking, Plk1 activity creates the phosphoepitope 3F3/2 and keeps the SAC activated (Ahonen et al., 2005). More recently, several researchers have argued that only interkinetochore tension is required (Maresca and Salmon, 2009; O'Connell et al., 2008; Uchida et al., 2009). Whatever the mechanism, it is clear that rearrangements at the kinetochore-microtubule interface signal the cell that anaphase can proceed.

Microtubule-Perturbing Drugs and Mitosis

The drugs taxol and nocodazole interfere with normal spindle dynamics, which are important for mitotic processes (discussed above in *The Mitotic Spindle and Microtubule Dynamics*). Taxol binds to β-tubulin subunits in the polymer, stabilizing the microtubule and preventing its depolymerization (Xiao et al., 2006). Nocodazole causes selective depolymerization of the spindle, while increasing the length and density of astral microtubules in a cell (Jordan et al., 1992). Because of their effects on the mitotic spindle, both cause mitotic arrest. Taxol at concentrations of 10-100 nM causes a metaphase arrest, and nocodazole at a concentration of 100 nM causes a prometaphase arrest (Rieder, 1999). Nocodazole also causes the detachment of kinetochores from the spindle and the associated relocation of Mad2 to the kinetochore (Waters et al., 1998),

and an 18-fold increase in merotely-associated chromosome lagging has been reported in cells recovering from a nocodazole block (Cimini et al., 2003). However, another study reported that microtubule-stabilizing drugs, but not microtubule-destabilizing drugs, caused an increase in aneuploidy (Chen and Horwitz, 2002).

Mitosis with Unreplicated Genomes

Treating cultured cells with caffeine to enter M phase before the completion of S phase was first announced as a tool for inducing premature chromosome condensation (Schlegel and Pardee, 1986). This strategy was refined to produce what became known as MUG cells (**m**itosis with **u**nreplicated **g**enomes) (Brinkley et al., 1988). The MUG procedure has been attempted in the human HeLa cell line (O'Connell et al., 2008), but most reports are from CHO cells. Details of the MUG protocol are described in Chapter III, *Creation of MUG Cells*.

MUG cells are created in two stages: first, the cells are temporarily arrested with hydroxyurea; then, the cell cycle is restarted by adding caffeine to the medium. Hydroxyurea is an inhibitor of ribonucleotide reductase, the enzyme that catalyzes the conversion of ribonucleotide triphosphates to dinucleotide triphosphates, providing the monomers for DNA synthesis. In the presence of hydroxyurea, the cell cycle stops when the pool of nucleotides falls below ordinary levels (Koç et al., 2004). Caffeine, as mentioned earlier, is an inhibitor of the ATM/ATR kinases that mediate the DNA damage response. Therefore, in the presence of caffeine, a cell with incompletely replicated DNA will enter M phase. An additional, unexplained effect of the MUG procedure is the separation of the chromatin from the kinetochores (Brinkley et al., 1988). Electron microscopy data show that some centromeric DNA remains associated with the

kinetochore, but the remainder of the chromatin is excluded from the mitotic spindle (Wise and Brinkley, 1997).

The kinetochores of MUG cells align at the metaphase plate and complete mitosis, which appears normal except for the absence of anaphase B (Johnson and Wise, 2010). However, the kinetochore number is approximately 2C, because S phase (when kinetochores are assembled) was interrupted. The precise number of kinetochores in the CHO cell line is unknown, but the modal chromosome number is usually reported as 2n = 22 (ATCC CCL-61).

Electron microscopy studies have revealed that MUG kinetochores have an unusual morphology and abundant unorthodox attachments to the spindle, perhaps facilitated by its detachment from the chromosome. The appearance of the kinetochore is generally described as curved, rather than the flat structure thought to be attached to the chromosome in untreated cells. Both lateral and end-on attachments are present, but end-on attachments are likely to be merotelic. Nonetheless, the characteristic trilaminar structure appears to be intact, and the kinetochore is competent to bind microtubules (Wise and Brinkley, 1997).

Spindle Assembly Checkpoint Satisfaction and Error Correction in MUG Cells

According to the prevailing model of anaphase initiation, replicated chromosomes align at the metaphase plate under tension. While MUG cell kinetochores can certainly align at the equator, if they are under tension, then their attachments are necessarily merotelic. In cultured cells not treated by the MUG procedure, merotelic attachments that are not corrected before anaphase are believed to cause lagging kinetochores in anaphase (Cimini et al., 2001). Furthermore, if merotely is unbalanced, i.e., the merotelically-

attached kinetochore has more microtubules bound to one pole than to the other, then the chromatids segregate normally. However, if merotely is balanced, with an equal number of microtubules from each pole converging on a single kinetochore, then that chromosome lags at the metaphase plate (Cimini et al., 2004). Clearly, MUG cell kinetochores aligned at the metaphase plate and under tension should have balanced merotelic attachments. This model predicts that these MUG kinetochores would also lag. No investigations into the phenomenon of lagging in MUG cells have been reported.

Another way to examine kinetochore distribution in MUG cells is to ask whether kinetochores are distributed equally to the two daughter cells (DCs). In such a study, Johnson and Wise concluded that the distribution was equal. In a cell with 22 kinetochores (the 2n modal number for the CHOK1 line), equal distribution of 11 kinetochores to each DC would produce a kinetochore distribution ratio (KDR) of 1.0. If one DC received one extra kinetochore, the KDR for that DCP would be 10/12, or 0.83; if a DC received two extra kinetochores, the KDR would be 9/13, or 0.69. Therefore, out of 20 DCPs, they seem to have observed one DCP with two errors, 11 DCPs with one error, and 9 DCPs with no errors (Johnson and Wise, 2010). Of course, in this context, an error is not the distribution of a chromatid to the same cell as its sister (as in untreated cells), but rather the failure to distribute the kinetochores equally. Nevertheless, the fact than very few distribution errors were observed in any given cell raises the possibility that this distribution is not random. If there is such a system, it does not work perfectly; the fact that more than half of the observed cells had errors makes this clear.

CHAPTER II

RESEARCH QUESTIONS

MUG cells have been reported to distribute kinetochores equally to the two cells of a daughter cell pair (DCP), with few exceptions, despite an abundance of merotelic kinetochore-microtubule attachments. This suggests the presence of an active error recognition and correction system. The general questions asked in this study were whether perturbing the cell's microtubule dynamics or kinetochore number would reduce the efficiency of its error correction mechanisms, either by reducing the kinetochore distribution ratio (KDR) or by increasing kinetochore lagging in the midbody of the DCP. The specific research questions were:

1) Does treatment with low-dose taxol alter the number of kinetochores that lag in the midbody of MUG DCPs?

2) Does treatment with low-dose nocodazole alter the number of kinetochores that lag in the midbody of MUG DCPs?

3) Does increasing the kinetochore number alter the number of kinetochores that lag in the midbody of MUG DCPs?

4) Does treatment with low-dose taxol alter the average KDR of MUG DCPs?

5) Does treatment with low-dose nocodazole alter the average KDR of MUG DCPs?

6) Does increasing the kinetochore number alter the average KDR of MUG DCPs?

CHAPTER III

MATERIALS AND METHODS

Cell Culture

Chinese hamster ovary (CHO-K1) cells were obtained from ATCC (CCL-61) and cultured in McCoy's 5A (Modified) Medium (Life Technologies #16600-082) with 10% fetal bovine serum (Life Technologies #16000-036) and 1% antibiotic-antimycotic (Life Technologies #15240-062) in 5% CO_2 at 37° C. All cells were grown from cell suspensions on flame-sterilized coverslips in sterile petri dishes. The cell suspensions were prepared from confluent cultures by trypsin release. Unless otherwise indicated, 100 µl of cell suspension was added to 10 ml of medium. The duration of the cell cycle in this line is estimated to be 12 hours: G1 (2 hours), S (7 hours), G2 (2 hours), and M (1 hour) (Wise and Brinkley, 1997).

The treatment conditions are abbreviated as follows:

- **CHO**: untreated CHO cells
- **MUG**: MUG cells not treated with additional drugs
- **TAX-1**: MUG cells treated with 1 nM taxol
- **TAX-5**: MUG cells treated with 5 nM taxol
- **NOC-25**: MUG cells treated with 25 nM nocodazole
- **NOC-50**: MUG cells treated with 50 nM nocodazole
- **MUG-4C**: 4C MUG cells

Creation of MUG Cells (MUG)

Cells to be treated with the MUG protocol (Brinkley et al., 1988) were cultured for 24 hours in 10 ml of medium to allow them to attach to the substrate. Hydroxyurea (Sigma #H-8627) was then added to a final concentration of 2 mM. After 20 hours, the medium was replaced with fresh medium containing 2 mM hydroxyurea and 5 mM caffeine (Sigma #C-0750). After 7 hours, coverslips were rinsed with 1X PBS, fixed for 10 minutes on ice in cold 100% methanol, and stored at 20° C (Johnson and Wise, 2010). When labeled with DAPI to label the DNA (described in *Fluorescence Antibody Labeling* below) and viewed with confocal microscopy, these cells were clearly distinguishable from untreated CHO cells (Figure 1) by their characteristic fragmented DNA (Figure 2). Such observations showed that virtually the entire population entered M phase without replication.

Creation of Taxol-Treated MUG Cells (TAX-1 and TAX-5)

The concentrations of taxol were chosen experimentally using untreated CHO cells, beginning with concentrations expected to alter microtubule dynamics in mammalian cells without inducing cell cycle arrest (Evans, 2009; Rieder, 1999). After the cells were attached to the coverslips, they were grown for 7 hours in medium containing 100 nM, 50 nM, 25 nM, 10 nM, 5 nM, 2 nM, or 1 nM taxol (Sigma #T-7402) dissolved in DMSO, and fixed in methanol as described above. The final concentration of DMSO in each treatment group was less than 0.5%. After fluorescence labeling with antibodies to tubulin and kinetochores (described in *Fluorescence Antibody Labeling* below), the cells were observed with fluorescence microscopy. All concentrations higher than 5 nM taxol produced cells with abnormal cytoskeletons and population-wide cell

cycle arrest. Cells treated with 5 nM, 2 nM, or 1 nM taxol were further evaluated with confocal microscopy (described in *Confocal Microscopy and Immunofluorescence* below) for the presence of daughter cell pairs (DCPs). Because DCPs were observed at all three concentrations, the 1 nM and 5 nM conditions were chosen for further observations, with the expectation that concentration-dependent differences would be more readily observed by comparing these groups than by comparing either with cells grown in 2 nM taxol.

Taxol-treated MUG cells were then created by adding 1 or 5 nM taxol along with 2 mM hydroxyurea and 5 mM caffeine, as described above in *Creation of MUG Cells* and incubating for 7 hours. Coverslips were fixed as described in *Creation of MUG Cells*.

Creation of Nocodazole-Treated MUG Cells (NOC-25 and NOC-50)

The concentrations of nocodazole were chosen experimentally using untreated CHO cells, beginning with concentrations expected to alter microtubule dynamics in mammalian cells without inducing cell cycle arrest (Evans, 2009; Rieder, 1999). After the cells were attached to the coverslips, they were grown for 7 hours in medium containing 2 μM, 1 μM, 500 nM, 200 nM, 100 nM, 50 nM, and 25 nM nocodazole (Sigma #M-1404) dissolved in DMSO, and fixed in methanol as described above. The final concentration of DMSO in each treatment group was less than 0.5%. After fluorescence labeling with antibodies to tubulin and kinetochores (described in *Fluorescence Antibody Labeling* below), the cells were observed with fluorescence microscopy. All concentrations higher than 100 nM nocodazole produced cells with abnormal cytoskeletons (usually one, but occasionally two, foci of short microtubules near the nucleus of each cell) and population-wide cell cycle arrest before the

establishment of a spindle. Cells treated with 100 nM, 50 nM, or 25 nM nocodazole were further evaluated with confocal microscopy (described in *Confocal Microscopy and Immunofluorescence* below) for the presence of daughter cell pairs (DCPs). DCPs were observed at all three concentrations, but were far less prevalent in the 100 nM nocodazole treatment group. (The differences in the numbers of DCPs among the three treatment groups were not quantified.) Therefore, the 25 and 50 nM conditions were chosen for further observations.

Nocodazole-treated MUG cells were then created by adding 25 or 50 nM nocodazole along with 2 mM hydroxyurea and 5 mM caffeine, as described above in *Creation of MUG Cells* and incubating for 7 hours. Coverslips were fixed as described in *Creation of MUG Cells*.

Creation of 4C MUG Cells (MUG-4C)

Treatment with cytochalasin D inhibits the formation of the cleavage furrow in cytokinesis, producing binucleate cells (Zieve, 1984). The conditions for cytochalasin D treatment were chosen experimentally using untreated CHO cells. After the cells were attached to the coverslips, they were grown for 15 hours (to allow for the completion of an entire cell cycle) in medium containing 5 μM, 2 μM, 1 μM, or 500 nM cytochalasin D (Sigma #C-8273) dissolved in DMSO, and fixed in methanol as described above. The final concentration of DMSO was less than 0.5%.

Light microscopy (without fluorescence antibody labeling) was used to confirm that the population was enriched in binucleate cells. (This was not quantified, although virtually all cells appeared binucleate.) While binucleate cells were observed in all conditions, 4C cells were most abundant in the 5 μM group. Two additional tests were

performed to confirm the creation of 4C cells in this treatment group. For these tests, coverslips were mounted on slides with a DAPI-containing mounting medium, to allow the visualization of the nuclei by fluorescence microscopy (described in *Fluorescence Antibody Labeling* below). First, the total nuclear volumes of 24 cells without cytochalasin D and 19 cells treated with cytochalasin D for 7 hours were measured (described in *Confocal Microscopy* and *Measurements* below). Both populations were asynchronous, but both the mean and the range of the total nuclear signal in the cytochalasin D-treated population were greater. However, because the signal in the untreated cells faded unusually quickly, a second type of measurement was performed. Using similar procedures, the largest cross-sectional area of the nucleus was measured in both populations. Nuclei in the untreated group (Figure 3) had a larger mean and range of area than in the cytochalasin D-treated group (Figure 4).

Populations enriched in 4C MUG cells were started with a 50 µl cell suspension, to prevent overcrowding on the coverslip during the additional incubation time required for the cytochalasin D treatment. Cells were allowed to attach to the coverslip, and cytochalasin D was added to the medium to a final concentration of 5 µM. After 15 hours of incubation, coverslips were rinsed with fresh medium to remove the cytochalasin D and then treated as described above in *Creation of MUG Cells*, beginning with the addition of 2 mM hydroxyurea.

Fluorescence Antibody Labeling

Coverslips were incubated with antibodies to label them for immunofluorescence. All antibody incubations were 30 minutes at 37° C, and coverslips were rinsed twice with 1X PBS after each step. Cells were blocked in a solution of 1% BSA, 0.1% Triton X-100,

and 0.2% sodium azide in PBS (Johnson and Wise, 2010). Primary antibodies were mouse anti-α-tubulin DM1A antibody (1:1000; Sigma #T-6199) and human anti-centromere (kinetochore) antibody [ACA] (1:10; Antibodies, Inc. #15-234). Secondary antibodies were Alexa Fluor® 568 goat anti-mouse (Invitrogen #A21124) and Alexa Fluor® 488 goat anti-human (Invitrogen #A11013), both 1:2000. After antibody labeling, coverslips were mounted on slides using Fluoroshield® with DAPI (Sigma #F-6057) to enable the visualization of DNA with fluorescence microscopy. Therefore, under fluorescence, kinetochores appeared green, microtubules red, and DNA blue. Each slide was assigned an alphanumeric code that could be retrieved after analysis but did not identify its condition during image acquisition. However, both 4C MUG cells (due to their large size) and untreated CHO cells (due to their intact nuclei) were recognizable by condition under the microscope. Slides were stored at 20° C.

Confocal Microscopy and Immunofluorescence

While four slides were prepared in each treatment condition, only one slide was required to obtain the necessary data for each condition. Each slide was surveyed in a consistent pattern to avoid observing a single DCP more than once. DCPs were identified by viewing the slide in the red channel through the microscope's ocular lens to observe microtubules organized into a midbody, signifying a DCP. The blue channel was used to verify fragmented chromatin consistent with MUG cell treatment. A DCP was excluded if its nucleus overlapped with another cell's, if it lay in a portion of the field that had been exposed to the laser during an earlier image acquisition, or if its kinetochores were difficult to see clearly through the ocular lens (such kinetochores were never clearly visualized in the acquired image). Otherwise, the first 20 DCPs observed were collected

for each condition. For the cytochalasin D-treated populations, small DCPs (i.e., those that required a digital zoom to fill the computer screen) were presumed to be 2C cells and were excluded. (The number of presumed 2C cells that was excluded was not recorded.) The microscope was focused on the plane with the brightest and most abundant kinetochores in the DCP, and this plane was used to optimize the green fluorescence signal (described in the following paragraph). Once the kinetochore signal was optimized, the first and last positions of the nucleus in the Z axis were marked, and a set of 0.5 μm-slices through the entire volume (a Z-stack) was collected (for an example, see Figure 5). Kinetochores are clearly visible with the channels separated (Figure 6).

Images were collected with a Zeiss Axiovert 200M confocal microscope with a plan apochromat 100x/1.4 oil immersion differential interference contrast objective lens, with the following acquisition settings: slice thickness = 0.5 μm, frame size 1024 x 1024; line step = 1; scan speed = 6 (pixel time = 3.2 μsec), and 2 images averaged per acquisition. The data depth was 12-bit, except for 5 of 20 DCPs in the MUG condition, 2 of 20 DCPs in the TAX-1 condition, and all DCPs in the cytochalasin D-treated group, which were collected at 8-bit, due to a computer setting error (see Table 1 for a listing of the 8-bit images). Laser and filter settings were the same for all acquisitions in a given channel: for red fluorescence, a long pass (LP) 560 nm filter; for green fluorescence, a band pass (BP) 505-530 nm filter; and for blue fluorescence, a BP 420-480 nm filter. Channel settings (pinhole, percent transmission, detector gain, and amplifier offset) were changed minimally, except in the green channel (kinetochores). Because of the kinetochores' small size (< 10 nm; see Figure 7 for an example), adjustments to the detector gain were required before the acquisition of each DCP to visualize them. To

further improve the visualization of the kinetochores, all images except from the 4C MUG condition were collected at a digital zoom of 2, enabling the necessary adjustments to the detector gain while minimizing the exposure of the sample to the lasers. Because the 4C MUG cells were so large, the entire DCP could not be viewed on the computer screen at a zoom of 2, and so images from that condition were acquired without zooming. Images were given a numerical code so that their condition was not obvious during image analysis.

Fluorescence Intensity Measurements

ImageJ software (Rasband, 1997-2014) was used to measure the fluorescence intensity of the **a**nti-**c**entromere **a**ntibody (ACA, the kinetochore signal) in each MUG daughter cell (DC). Although intact kinetochores were clearly visible in all images, additional green background fluorescence was usually also present. Furthermore, since the DNA was fragmented, the MUG cell nucleus (which defines the area in which the kinetochores can be found) was not clearly identifiable. To measure the kinetochore signal consistently, the smallest area containing the entire blue fluorescence signal (DNA), which was better defined than the region of green signal (kinetochores), was circumscribed. The total kinetochore fluorescence intensity varied considerably among DCPs (see Figure 8), so setting a threshold below which the green signal would be deemed an artifact would have required an arbitrary judgment and would have been difficult to do consistently across all DCPs. Therefore, to measure the total ACA signal, the smallest region that included the entire DNA signal was manually circumscribed, and the ACA signal intensity within this boundary (total integrated density in ImageJ) was measured for each slice of each DCP of the Z-stack. The total signal intensity was

calculated for each DCP, and a kinetochore distribution ratio (KDR) was calculated. Because the choice of numerator and denominator in the ratio is completely arbitrary, the inverse was calculated for ratios less than 1, such that for analyses, all ratios were greater than 1.

Coding of Lagging Kinetochores

The number of DCPs in each condition with one or more kinetochores lagging in the midbody was coded dichotomously by visual inspection of the image files. The midbody was generally visible in only a single slice of a given DCP. This region was manually circumscribed, and all slices within this defined area were surveyed for kinetochores. Although nonspecific ACA signal was commonly observed in the nuclear region, the midbody was generally free of such interfering signal, and when ACA signals were observed in the midbody, they were round and could be confidently interpreted to represent kinetochores (Figures 9 and 10).

In an attempt to more carefully describe the phenomenon of lagging kinetochores, the midbody was circumscribed as described in the previous paragraph, and the intensity of ACA signal in the midbody (ACA_M) of each DCP was measured (as described in *Fluorescence Intensity Measurements*). The ACA_M was divided by the total ACA signal in the entire DCP (ACA_T) to determine the percentage of the ACA signal that was contributed by the midbody ($\% = ACA_M / ACA_T$). However, these measurements were often inconsistent with visual inspection of the images. As shown in Table 2, there is no relationship between these quantitative measurements and the dichotomous data collected for untreated CHO cells.

Statistical Analyses

Analysis of variance (ANOVA) was used to compare the KDRs of the treatment groups. The data analysis for this paper was generated using SAS software. Copyright, SAS Institute Inc. SAS and all other SAS Institute Inc. product or service names are registered trademarks or trademarks of SAS Institute Inc., Cary, NC, USA.

Table 1 Daughter Cell Pairs Collected As 8-Bit Images

Condition	Daughter Cell Pair Numbers
TAX-1	19-20
MUG	16-20
MUG-4C	1-20

Table 2 Quantitative and Dichotomous Data on Lagging Kinetochores in MUG Cells

Daughter Cell Pair	Percentage of Kinetochore Signal in Midbody	Lagging (0=no, 1=yes)
11	0.0094	0
3	0.0105	1
1	0.0113	0
16	0.0116	0
5	0.0130	0
4	0.0136	0
13	0.0143	0
2	0.0159	0
7	0.0198	1
12	0.0212	0
6	0.0224	0
10	0.0226	0
15	0.0246	0
18	0.0376	0
19	0.0395	0
9	0.0475	0
14	0.0495	0
20	0.0588	0
17	0.0596	0
8	0.0907	1

There is no relationship between the percentage of kinetochore signal in the midbody of MUG cells and lagging as observed by visual inspection of the image. CHO cells were grown on coverslips in medium containing 2 mM hydroxyurea and 5 mM caffeine to produce 2C MUG cells. Cells were fixed on coverslips in methanol and mounted on slides with a medium containing DAPI® to visualize nuclei. A confocal microscope with a 1.4 NA / 100x plan apochromat lens was used to obtain a Z-stack, and ImageJ software was used to measure the fluorescence intensity of the kinetochore signal in both cells of the daughter cell pair. Data in the table are sorted by increasing percentage of kinetochore signal in the midbody (column 2).

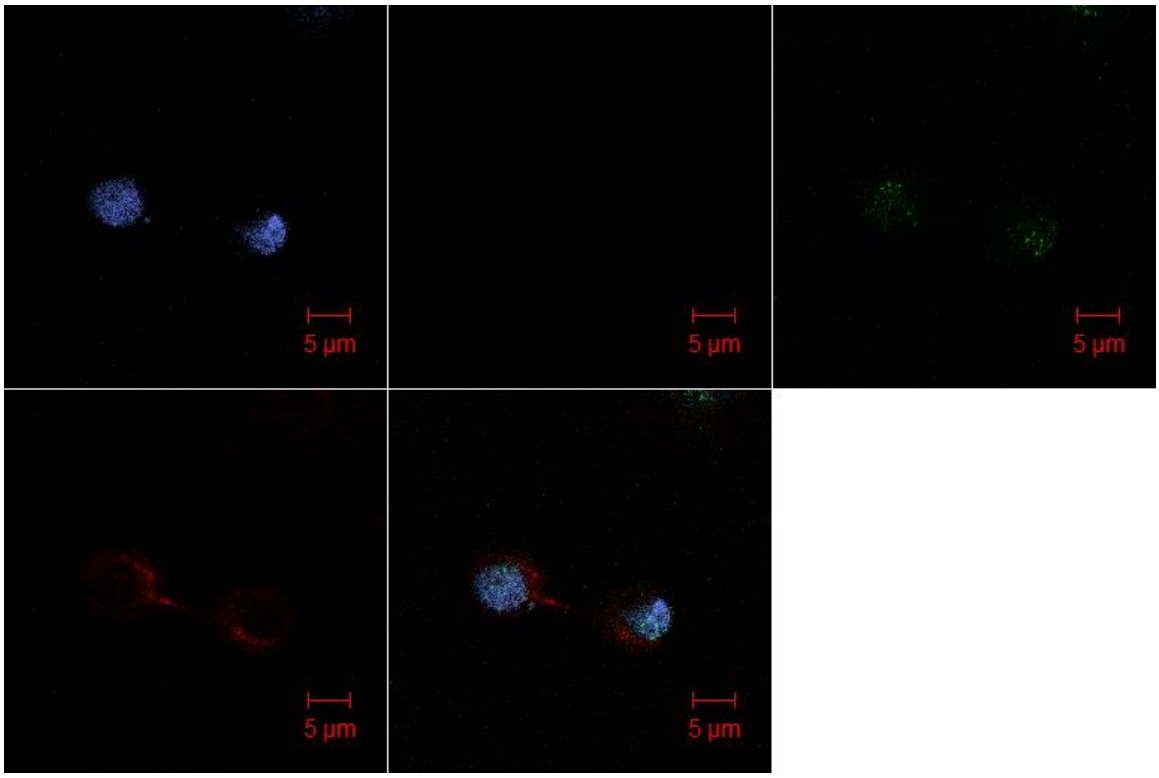

Figure 1 A Confocal Micrograph of a CHO Daughter Cell Pair

A single slice from an untreated CHO daughter cell pair shows intact nuclei. CHO cells were grown on coverslips, fixed in methanol, labeled with fluorescent antibodies, and mounted on slides with a medium containing DAPI®. A confocal microscope with a 1.4 NA / 100x plan apochromat lens was used to obtain a Z-stack. Microtubules (red), kinetochores (green), DNA (blue). Microtubules are only faintly visible in this slice.

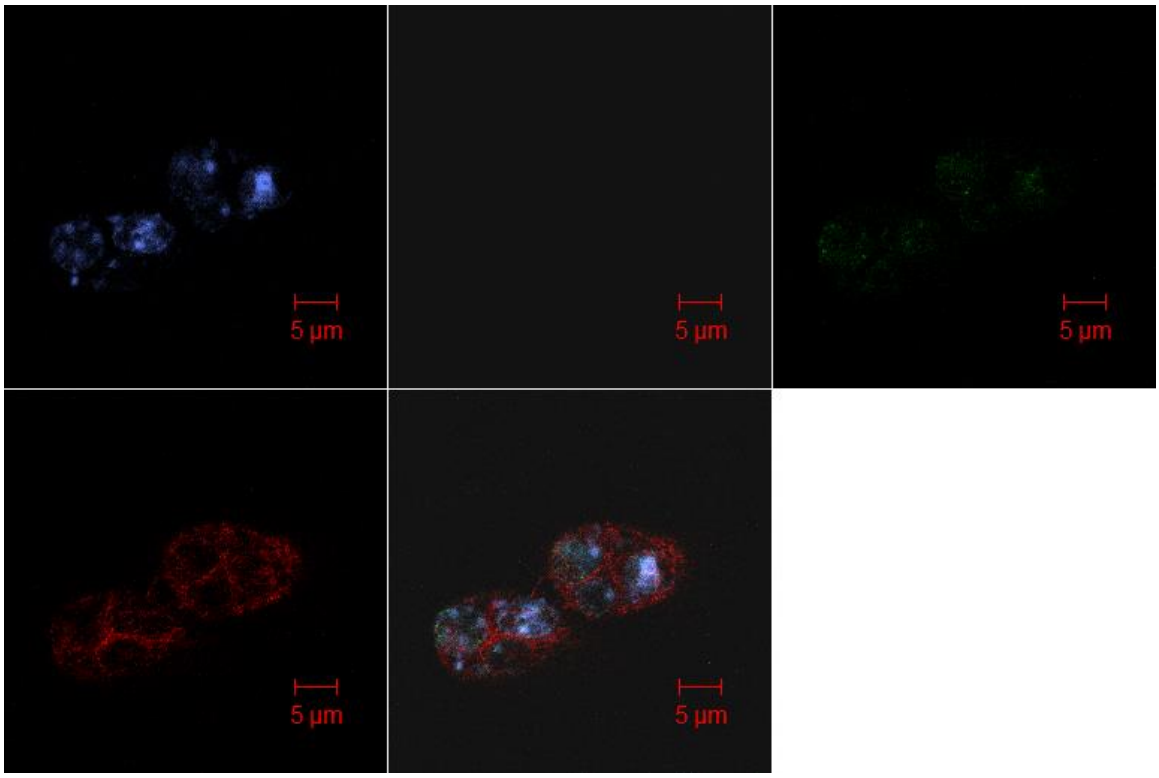

Figure 2 A Confocal Micrograph of a MUG Daughter Cell Pair

A single slice from a MUG daughter cell pair shows fragmented chromatin. CHO cells were grown on coverslips with in medium containing 2 mM hydroxyurea and 5 mM caffeine to produce MUG cells. Cells were fixed on coverslips in methanol, labeled with fluorescent antibodies, and mounted on slides with a medium containing DAPI®. A confocal microscope with a 1.4 NA / 100x plan apochromat lens was used to obtain a Z-stack. Microtubules (red), kinetochores (green), DNA (blue). Kinetochores are not visible in this slice.

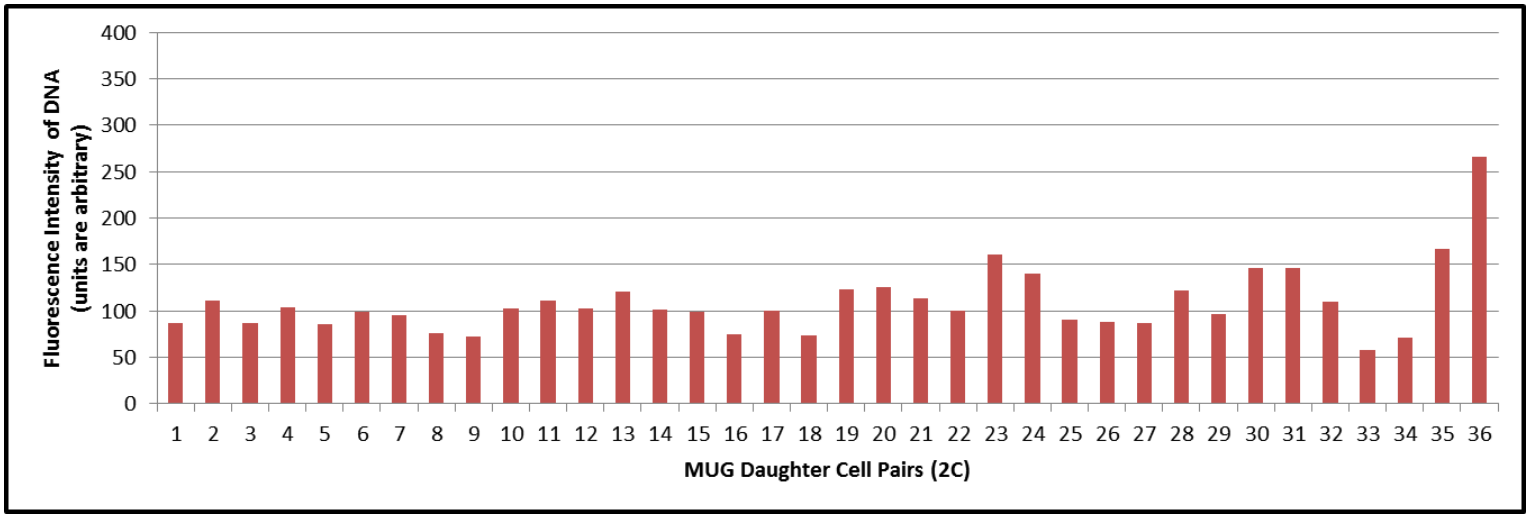

Figure 3 Fluorescence Intensity of DNA in 2C MUG Cells

CHO cells were grown on coverslips in medium containing 2 mM hydroxyurea and 5 mM caffeine to produce 2C MUG cells. Cells were fixed on coverslips in methanol and mounted on slides with a medium containing DAPI® to visualize nuclei. A confocal microscope with a 1.4 NA / 100x plan apochromat lens was used to obtain a Z-stack. A random sample of 36 cells was chosen from a coverslip, and ImageJ software was used to measure the fluorescence intensity of the largest slice through the nucleus of each cell. The fluorescence intensity of each daughter cell pair is plotted individually for each of 36 cells. Daughter cell pair #36 is probably the product of a spontaneously-generated 4C cell. Units of fluorescence intensity are arbitrary.

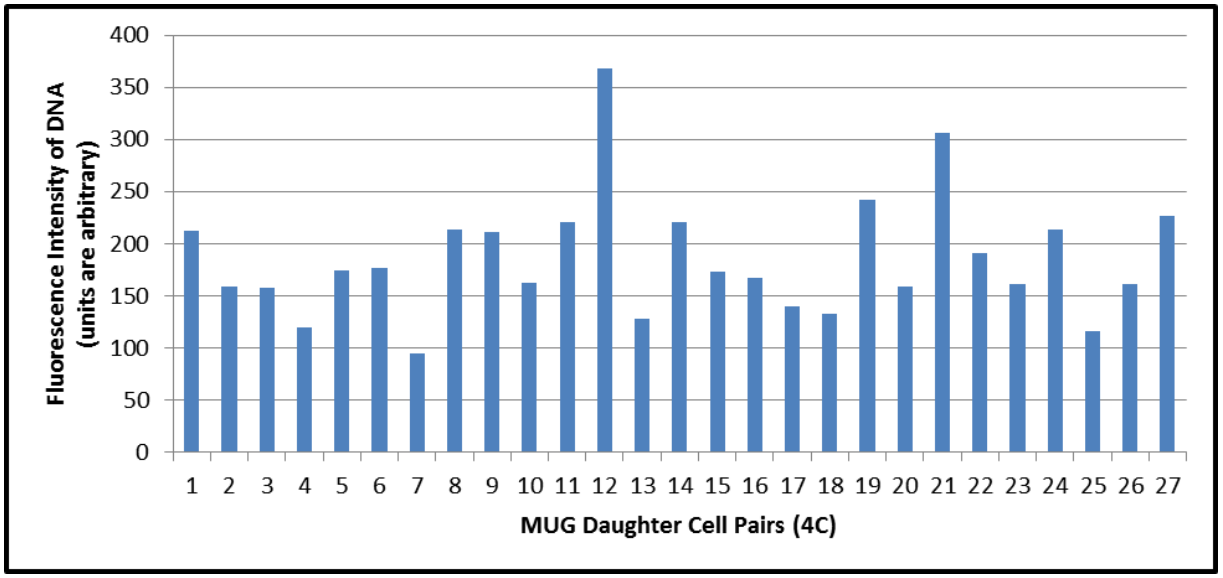

Figure 4 Fluorescence Intensity of DNA in 4C MUG Cells

CHO cells were grown on coverslips with 5 μM cytochalasin D to create 4C cells and then treated with 2 mM hydroxyurea and 5 mM caffeine to produce 4C MUG cells. Cells were fixed on coverslips in methanol and mounted on slides with a medium containing DAPI® to visualize nuclei. A confocal microscope with a 1.4 NA / 100x plan apochromat lens was used to obtain a Z-stack. A random sample of 27 cells was chosen from a coverslip, and ImageJ software was used to measure the fluorescence intensity of the largest slice through the nucleus of each cell. The fluorescence intensity of each daughter cell pair is plotted individually for each of 27 cells. As seen in the figure, not all cells in the population appear to be 4C. Therefore, large cells were chosen for kinetochore distribution analyses. Units of fluorescence intensity are arbitrary.

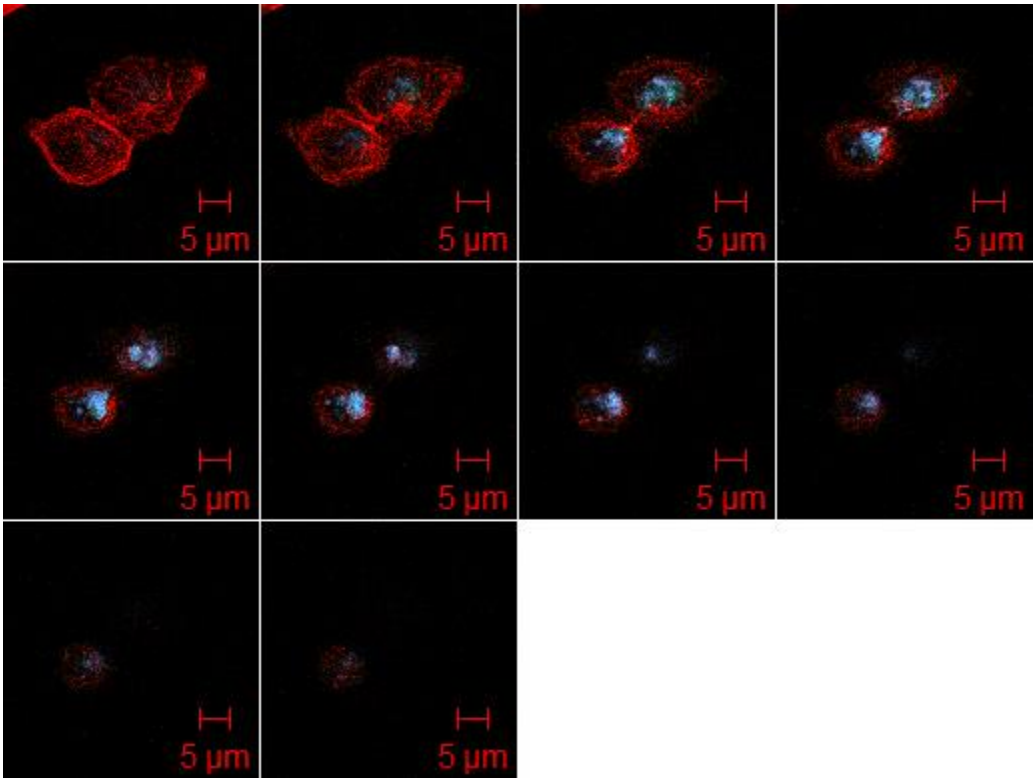

Figure 5 A Confocal Micrograph (Z-stack) of a Nocodazole-Treated Daughter Cell Pair

CHO cells were grown on coverslips with in medium containing 2 mM hydroxyurea and 5 mM caffeine to produce MUG cells. Cells were fixed on coverslips in methanol, labeled with fluorescent antibodies, and mounted on slides with a medium containing DAPI®. A confocal microscope with a 1.4 NA / 100x plan apochromat lens was used to obtain a Z-stack (slice thickness 0.5 µm). The third slice (1.00 µm) is reproduced in Figure 6 with the channels separate. Microtubules (red), kinetochores (green), DNA (blue).

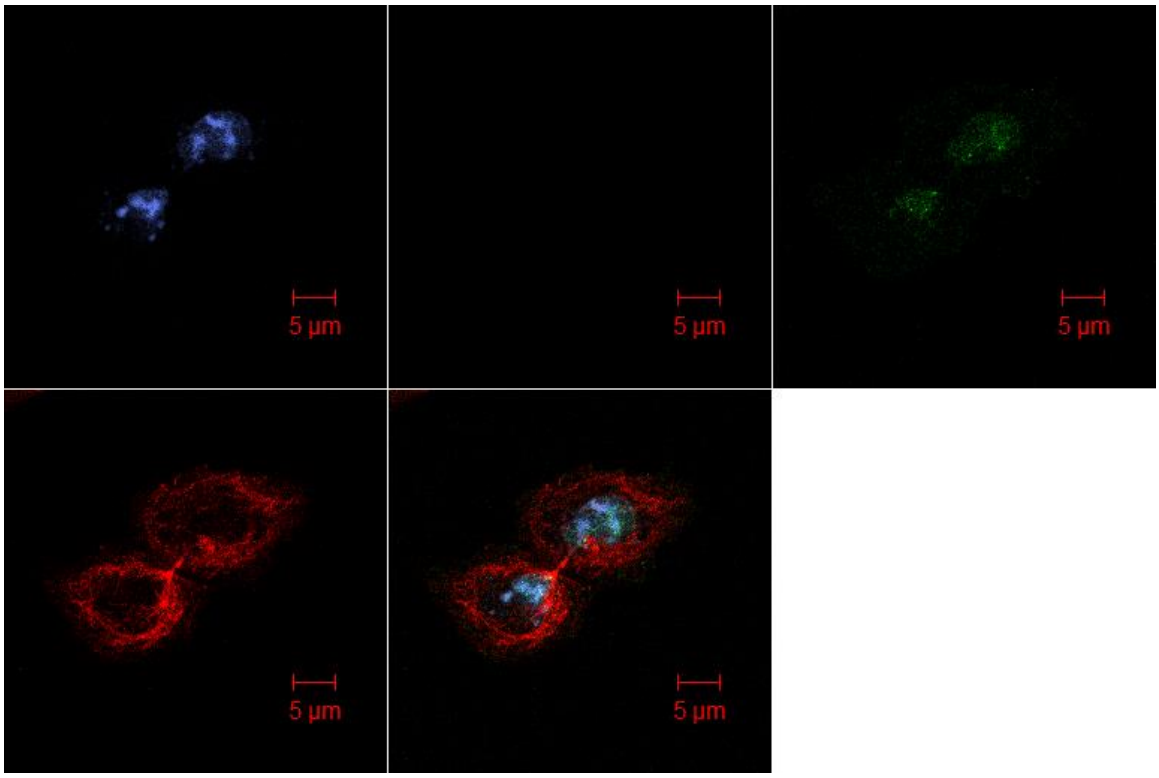

Figure 6 A Confocal Micrograph (Single Slice) of a Nocodazole-Treated Daughter Cell Pair

The third slice of the same nocodazole-treated daughter cell pair seen in Figure 5 is reproduced here to highlight kinetochores. CHO cells were grown on coverslips with in medium containing 2 mM hydroxyurea, 5 mM caffeine, and 25 nM nocodazole to produce nocodazole-treated MUG cells. Cells were fixed on coverslips in methanol, labeled with fluorescent antibodies, and mounted on slides with a medium containing DAPI®. A confocal microscope with a 1.4 NA / 100x plan apochromat lens was used to obtain a Z-stack. Microtubules (red), kinetochores (green), DNA (blue).

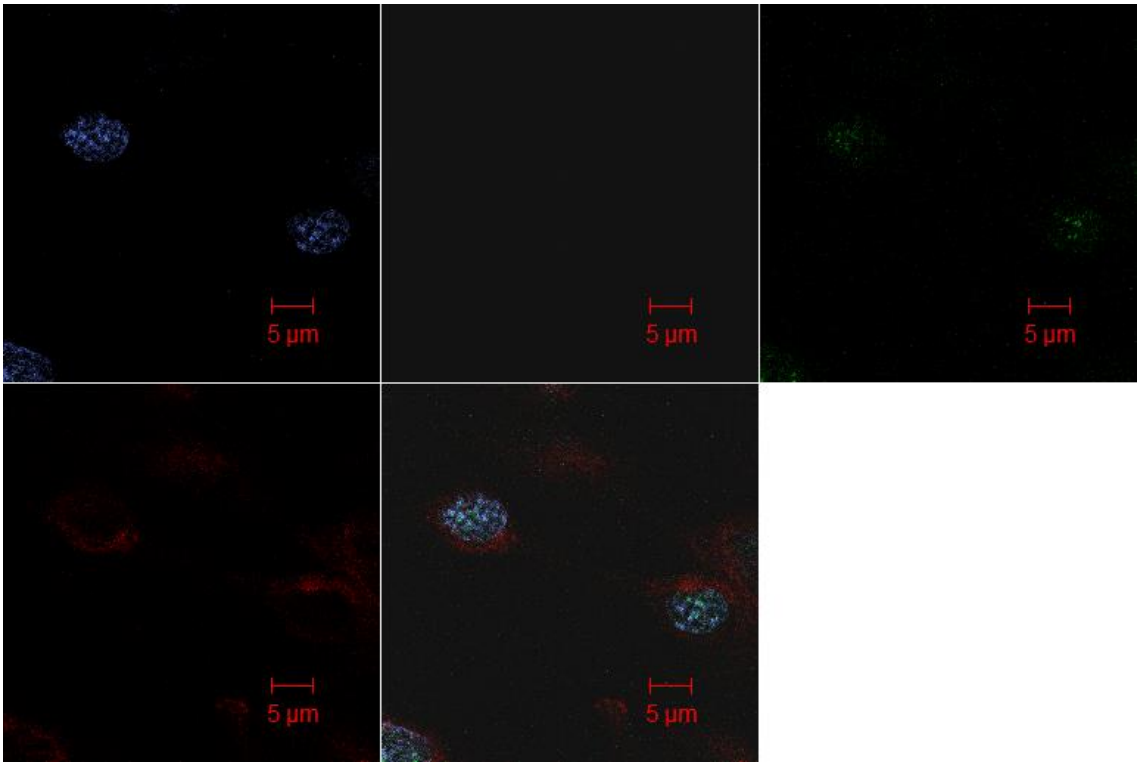

Figure 7 A Confocal Micrograph (Single Slice) of a CHO Daughter Cell Pair

A single slice of a CHO daughter cell pair demonstrates kinetochore size. CHO cells were grown on coverslips in medium containing 2 mM hydroxyurea and 5 mM caffeine. Cells were fixed on coverslips in methanol, labeled with fluorescent antibodies, and mounted on slides with a medium containing DAPI®. A confocal microscope with a 1.4 NA / 100x plan apochromat lens was used to obtain a Z-stack. Microtubules (red), kinetochores (green), DNA (blue).

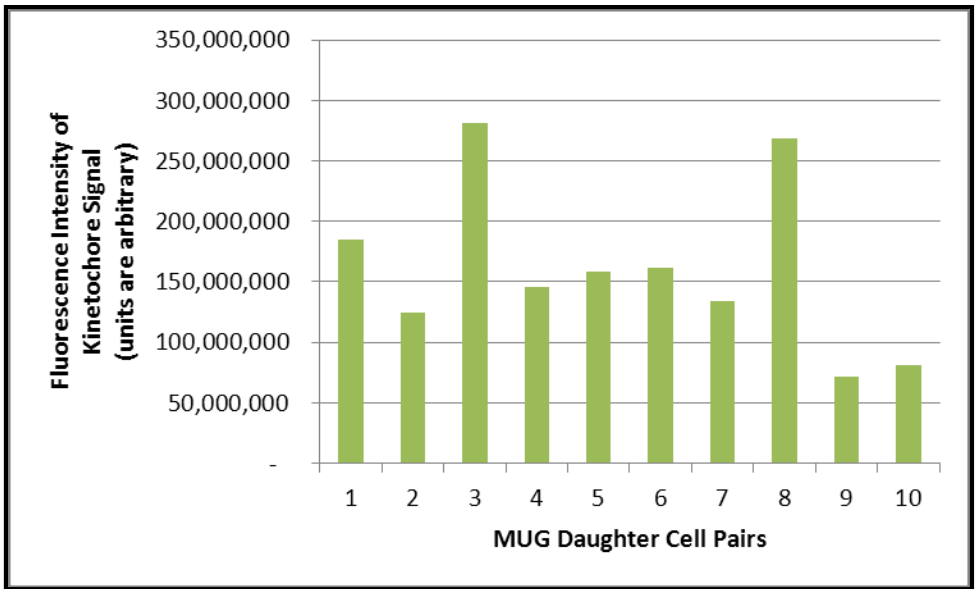

Figure 8 Fluorescence Intensity of Kinetochore Signal in MUG Cells

The fluorescence intensity of kinetochore signal in MUG cells is variable. CHO cells were grown on coverslips in medium containing 2 mM hydroxyurea and 5 mM caffeine to produce MUG cells. Cells were fixed on coverslips in methanol and mounted on slides with a medium containing DAPI® to visualize nuclei. A confocal microscope with a 1.4 NA / 100x plan apochromat lens was used to obtain a Z-stack. ImageJ software was used to measure the total fluorescence intensity of the kinetochore signal from 10 cells. Units of fluorescence intensity are arbitrary.

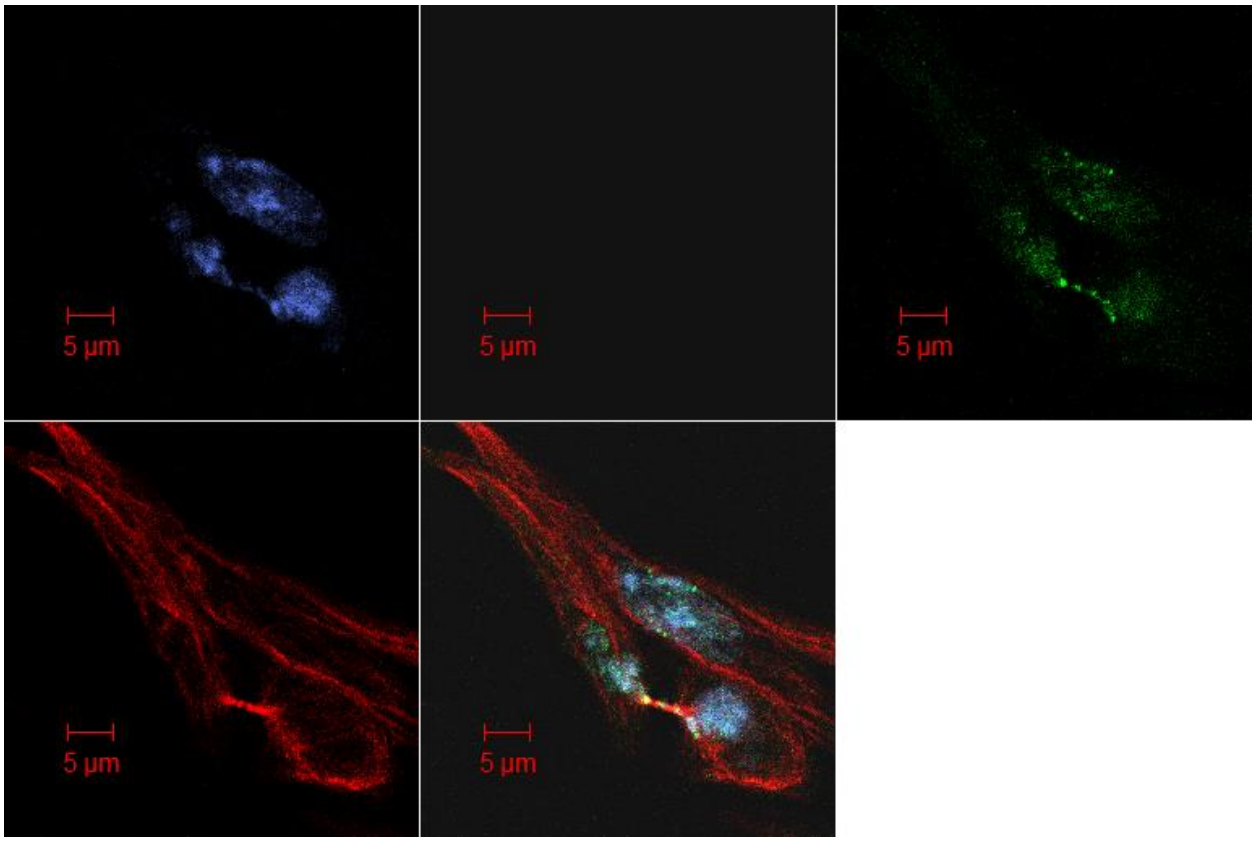

Figure 9 The First Slice of a Nocodazole-Treated Daughter Cell Pair with Lagging Kinetochores

A slice of a nocodazole-treated daughter cell pair shows that lagging kinetochores are clearly defined. CHO cells were grown on coverslips with in medium containing 2 mM hydroxyurea, 5 mM caffeine, and 25 nM nocodazole to produce nocodazole-treated MUG cells. Cells were fixed on coverslips in methanol, labeled with fluorescent antibodies, and mounted on slides with a medium containing DAPI®. A confocal microscope with a 1.4 NA / 100x plan apochromat lens was used to obtain a Z-stack. Microtubules (red), kinetochores (green), DNA (blue). The first of two consecutive slices (see Figure 10 for second slice).

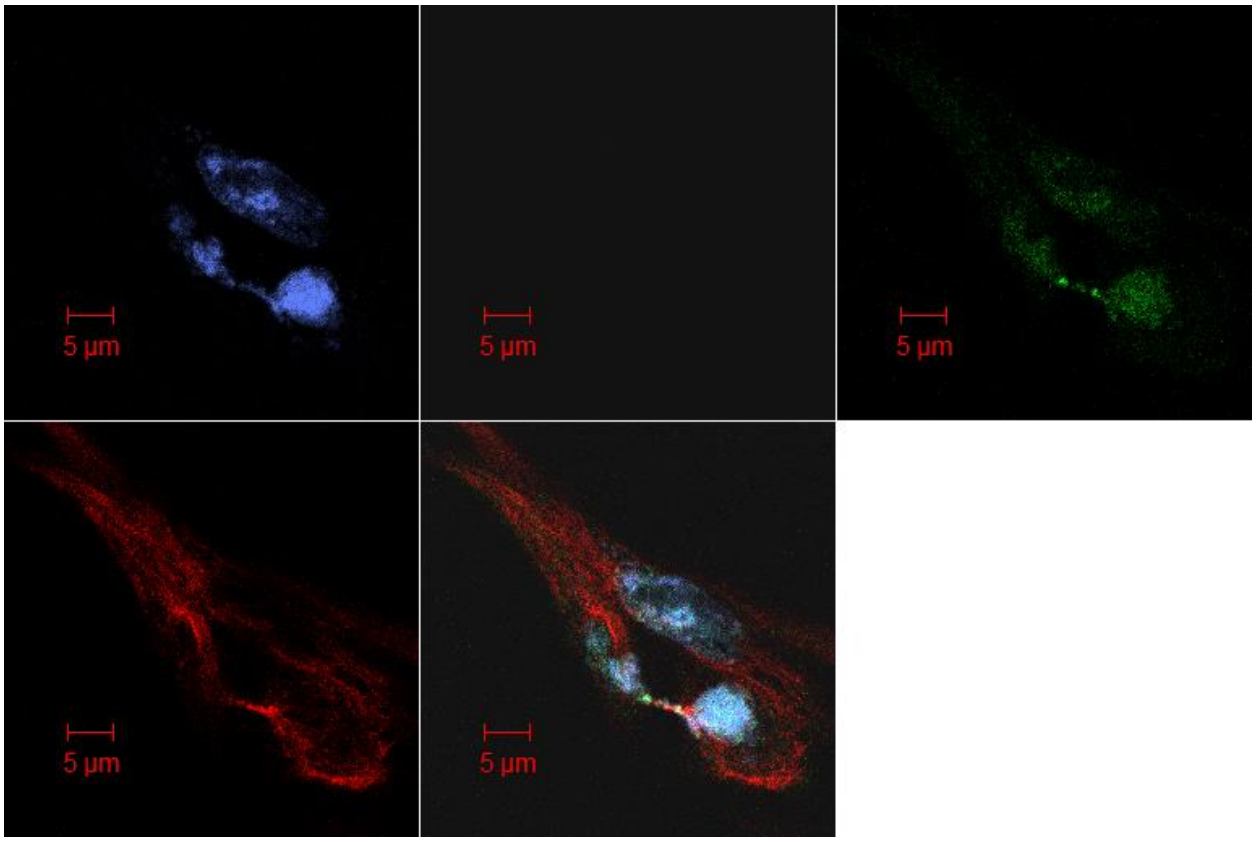

Figure 10 The Second Slice of a Nocodazole-Treated Daughter Cell Pair with Lagging Kinetochores

A slice of a nocodazole-treated daughter cell pair shows that lagging kinetochores are clearly defined. CHO cells were grown on coverslips with in medium containing 2 mM hydroxyurea, 5 mM caffeine, and 25 nM nocodazole to produce nocodazole-treated MUG cells. Cells were fixed on coverslips in methanol, labeled with fluorescent antibodies, and mounted on slides with a medium containing DAPI®. A confocal microscope with a 1.4 NA / 100x plan apochromat lens was used to obtain a Z-stack. Microtubules (red), kinetochores (green), DNA (blue). The second of two consecutive slices (see Figure 9 for first slice).

CHAPTER IV

RESULTS

Baseline Measurements of Lagging Kinetochores

To identify the baseline lagging frequency, Z-stacks of 20 MUG and 20 control daughter cell pairs were scored for the presence of ACA fluorescence in the midbody. Two of 20 unperturbed CHO (10%) and three of 20 MUGs (15%) had lagging kinetochores. Data on lagging kinetochores are summarized in Table 3.

Effects of Taxol on the Percentage of Cells with Lagging Kinetochores

Cells treated with 1 or 5 nM taxol were also scored for the presence of ACA fluorescence in the midbody. As in the two nocodazole treatment groups, 10 of 20 (50%) cells treated with 5 nM taxol showed lagging kinetochores. Only 3 of 20 (15%) cells treated with 1 nM taxol showed lagging kinetochores, as in the unperturbed MUG group.

Effects of Nocodazole on the Percentage of Cells with Lagging Kinetochores

Cells treated with 25 or 50 nM nocodazole were scored as above for the presence of ACA fluorescence in the midbody and compared with MUG cells cultured without microtubule-perturbing drugs. Nine of 20 (45%) and 10 of 20 (50%) cells treated with 25 and 50 nM nocodazole, respectively, had lagging kinetochores. Therefore, cells treated with nocodazole were approximately three times as likely as untreated MUGs to display lagging kinetochores.

Effects of Kinetochore Number on the Percentage of Cells with Lagging Kinetochores

Z-stacks of 20 MUG cells treated with cytochalasin D to produce cells with the 4C kinetochore number were scored for the presence of ACA fluorescence in the midbody and compared with 2C MUG cells. Six of 20 (30%) 4C MUG cells had lagging kinetochores, meaning that lagging was observed twice as frequently in 4C as in 2C MUG cells.

Average Effects of Treatments on Kinetochore Distribution Ratios

To establish a baseline KDR for DCPs of cultured CHO cells, 20 cell pairs were examined. When necessary, the inverse of the ratio was taken, so that all ACA fluorescence intensity values were greater than 1. The average ratio was 1.11, with a range from 1.02 to 1.31 (Table 4). By contrast, the KDRs for DCPs of MUG cells treated with no additional drugs, MUGs treated with 1 nM taxol, MUGs treated with 25 nM nocodazole, or 4C MUGs were higher, meaning that the distribution of the kinetochores to the two DCs was less equal in these conditions. KDRs for DCPs of MUGs treated with 5 nM taxol or MUGs treated with 50 nM nocodazole were closer to the average KDR of controls ($p = 0.02$). The results of an ANOVA analysis are summarized in Table 5.

Effects of Treatments on the Kinetochore Distribution Ratios of Individual Cells

Across all MUG conditions, between 3 and 9 of 20 DCPs (15-45%) had KDRs greater than 1.31, the maximum KDR observed in the CHO condition. Therefore, in each MUG condition, at least 55% of cells had KDRs that were comparable to controls. In the conditions in which microtubule-perturbing drugs were used in different concentrations, fewer DCPs with KDRs outside the range of controls were found with the higher

concentration of drug: 9 of 20 (45%) in NOC-25 vs. 6 of 20 (30%) in NOC-50, and 6 of 20 (30%) in TAX-1 vs. 3 of 20 (15%) in TAX-5. KDRs for each treatment group are shown in Figures 11-17.

Table 3 Frequency of Lagging Kinetochores by Condition

Condition (n = 20 for each)	Number of Cells with Lagging Kinetochores	Percentage of Cells with Lagging Kinetochores
CHO	2	10
MUG	3	15
TAX-1	3	15
TAX-5	10	50
NOC-25	9	45
NOC-50	10	50
MUG-4C	6	30

CHO cells were grown on coverslips in medium containing 2 mM hydroxyurea, 5 mM caffeine, and additional drugs as indicated for the condition (taxol, nocodazole, or cytochalasin D). Cells were fixed on coverslips in methanol, labeled with fluorescent antibodies, and mounted on slides with a medium containing DAPI®. A confocal microscope with a 1.4 NA / 100x plan apochromat lens was used to obtain a Z-stack. Microtubules (red), kinetochores (green), DNA (blue). Lagging kinetochores were defined as those in or directly adjacent to the midbody. Lagging was coded by visual inspection of images. See *Methods* for details of cell culture.

Table 4 Mean Kinetochore Distribution Ratio by Condition

Condition (n = 20 for each)	Mean Kinetochore Distribution Ratio
CHO	1.11
MUG	1.32
TAX-1	1.31
TAX-5	1.19
NOC-25	1.39
NOC-50	1.25
MUG-4C	1.28

CHO cells were grown on coverslips in medium containing 2 mM hydroxyurea, 5 mM caffeine, and additional drugs as indicated for the condition (taxol, nocodazole, or cytochalasin D). Cells were fixed on coverslips in methanol, labeled with fluorescent antibodies, and mounted on slides with a medium containing DAPI®. A confocal microscope with a 1.4 NA / 100x plan apochromat lens was used to obtain a Z-stack. Microtubules (red), kinetochores (green), DNA (blue). ImageJ software was used to measure the total fluorescence intensity of kinetochore signal in each member of each daughter cell pair, and a kinetochore distribution ratio was calculated for each pair. For ratios less than 1, the inverse was taken so that all ratios used for analysis were greater than 1. See *Methods* for the details of cell culture procedures.

Table 5 Results of Analysis of Variance on Kinetochore Distribution Ratios

T grouping			Mean Kinetochore Distribution Ratio	Condition
	A		1.39	NOC-25
	A			
B	A		1.32	MUG
B	A			
B	A		1.31	TAX-1
B	A			
B	A		1.28	MUG-4C
B	A			
B	A	C	1.25	NOC-50
B		C		
B		C	1.19	TAX-5
		C		
		C	1.11	CHO

Mean kinetochore distribution ratios were analyzed by condition. Overlapping groups make the results difficult to interpret, but the cells with higher concentrations of microtubule-perturbing drugs are grouped with untreated CHO cells, and cells treated with lower concentrations of microtubule-perturbing drugs are grouped with MUG cells ($p=0.02$).

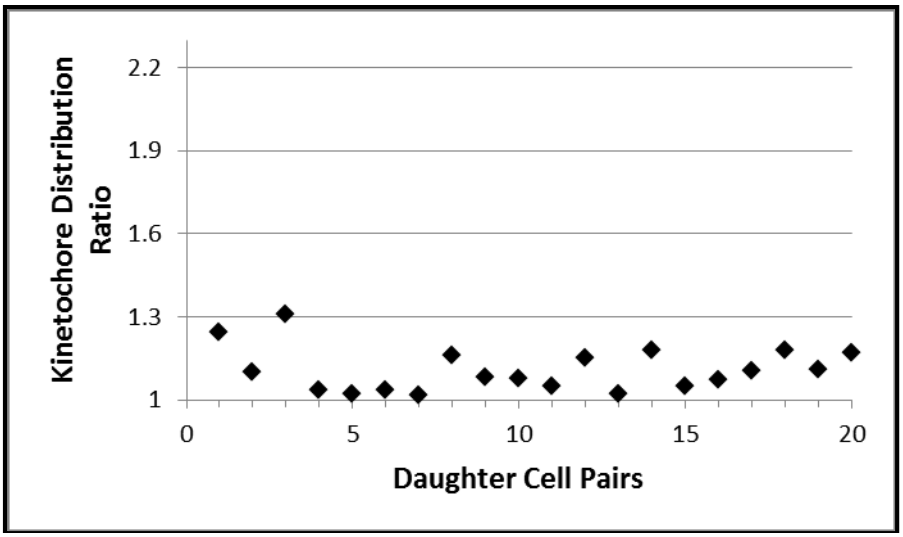

Figure 11 Kinetochore Distribution Ratios for CHO Cells

CHO cells were grown on coverslips, fixed in methanol, labeled with fluorescent antibodies, and mounted on slides with a medium containing DAPI®. A confocal microscope with a 1.4 NA / 100x plan apochromat lens was used to obtain a Z-stack. Microtubules (red), kinetochores (green), DNA (blue). ImageJ software was used to measure the total fluorescence intensity of kinetochore signal in each member of each daughter cell pair, and a kinetochore distribution ratio was calculated for each pair. For ratios less than 1, the inverse was taken so that all ratios used for analysis were greater than 1.

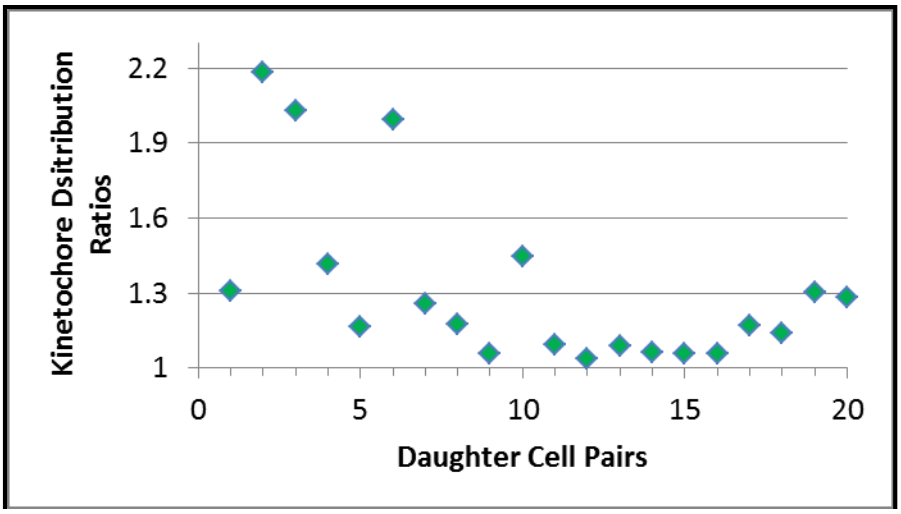

Figure 12 Kinetochore Distribution Ratios for MUG Cells

CHO cells were grown on coverslips in medium containing 2 mM hydroxyurea and 5 mM caffeine to produce MUG cells. Cells were then fixed in methanol, labeled with fluorescent antibodies, and mounted on slides with a medium containing DAPI®. A confocal microscope with a 1.4 NA / 100x plan apochromat lens was used to obtain a Z-stack. Microtubules (red), kinetochores (green), DNA (blue). ImageJ software was used to measure the total fluorescence intensity of kinetochore signal in each member of each daughter cell pair, and a kinetochore distribution ratio was calculated for each pair. For ratios less than 1, the inverse was taken so that all ratios used for analysis were greater than 1.

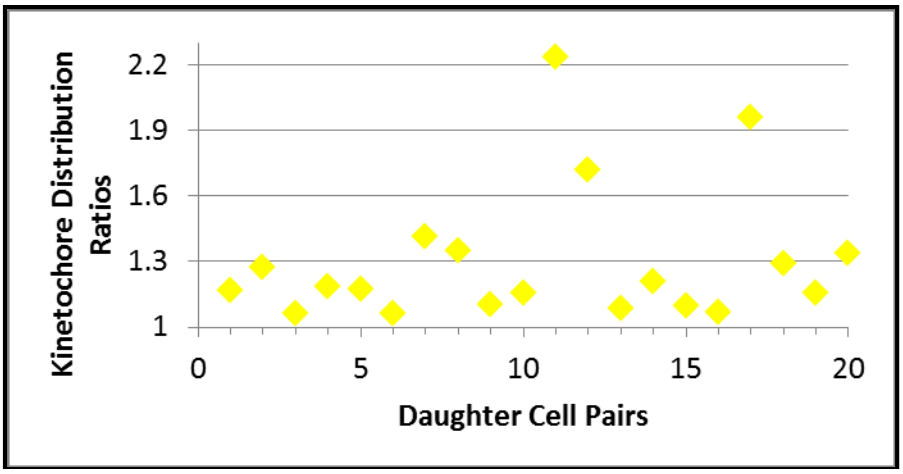

Figure 13 Kinetochore Distribution Ratios for Cells Treated with 1 nM Taxol

CHO cells were grown on coverslips in medium containing 2 mM hydroxyurea, 5 mM caffeine, and 1 nM taxol to produce taxol-treated MUG cells. Cells were then fixed in methanol, labeled with fluorescent antibodies, and mounted on slides with a medium containing DAPI®. A confocal microscope with a 1.4 NA / 100x plan apochromat lens was used to obtain a Z-stack. Microtubules (red), kinetochores (green), DNA (blue). ImageJ software was used to measure the total fluorescence intensity of kinetochore signal in each member of each daughter cell pair, and a kinetochore distribution ratio was calculated for each pair. For ratios less than 1, the inverse was taken so that all ratios used for analysis were greater than 1.

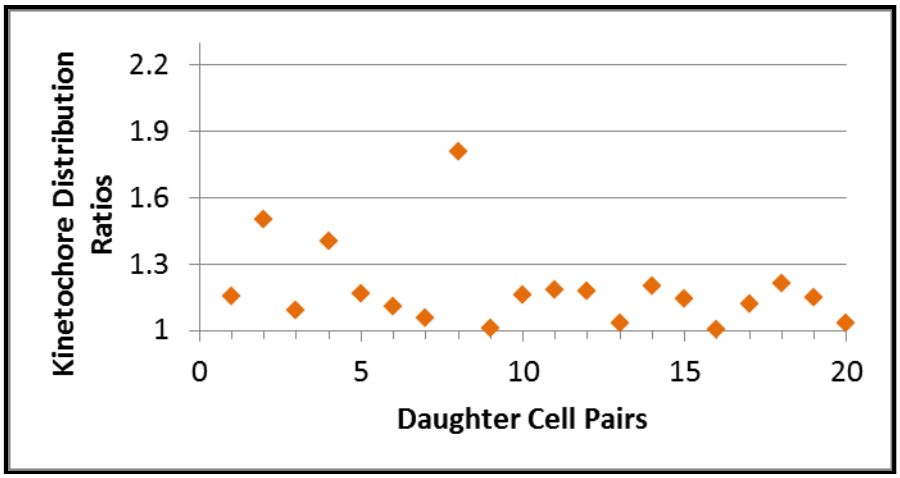

Figure 14 Kinetochore Distribution Ratios for Cells Treated with 5 nM Taxol

CHO cells were grown on coverslips in medium containing 2 mM hydroxyurea, 5 mM caffeine, and 5 nM taxol to produce taxol-treated MUG cells. Cells were then fixed in methanol, labeled with fluorescent antibodies, and mounted on slides with a medium containing DAPI®. A confocal microscope with a 1.4 NA / 100x plan apochromat lens was used to obtain a Z-stack. Microtubules (red), kinetochores (green), DNA (blue). ImageJ software was used to measure the total fluorescence intensity of kinetochore signal in each member of each daughter cell pair, and a kinetochore distribution ratio was calculated for each pair. For ratios less than 1, the inverse was taken so that all ratios used for analysis were greater than 1.

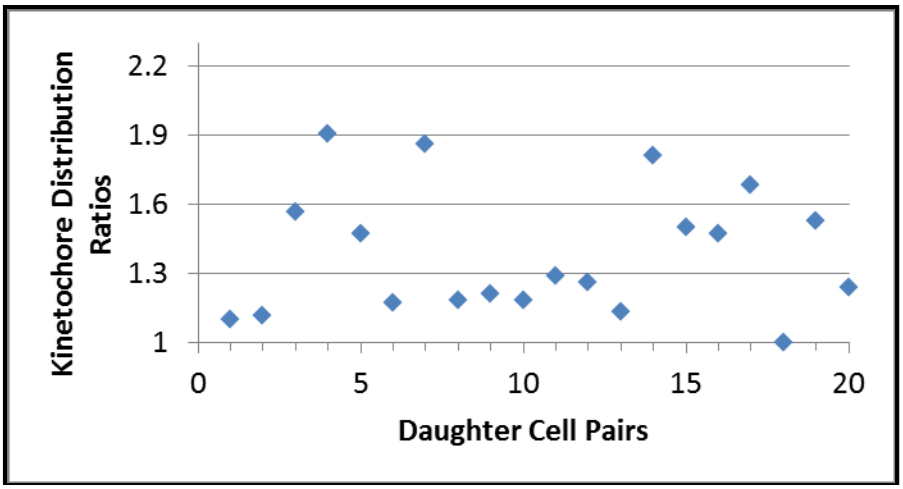

Figure 15 Kinetochore Distribution Ratios for Cells Treated with 25 nM Nocodazole

CHO cells were grown on coverslips in medium containing 2 mM hydroxyurea, 5 mM caffeine, and 25 nM nocodazole to produce nocodazole-treated MUG cells. Cells were then fixed in methanol, labeled with fluorescent antibodies, and mounted on slides with a medium containing DAPI®. A confocal microscope with a 1.4 NA / 100x plan apochromat lens was used to obtain a Z-stack. Microtubules (red), kinetochores (green), DNA (blue). ImageJ software was used to measure the total fluorescence intensity of kinetochore signal in each member of each daughter cell pair, and a kinetochore distribution ratio was calculated for each pair. For ratios less than 1, the inverse was taken so that all ratios used for analysis were greater than 1.

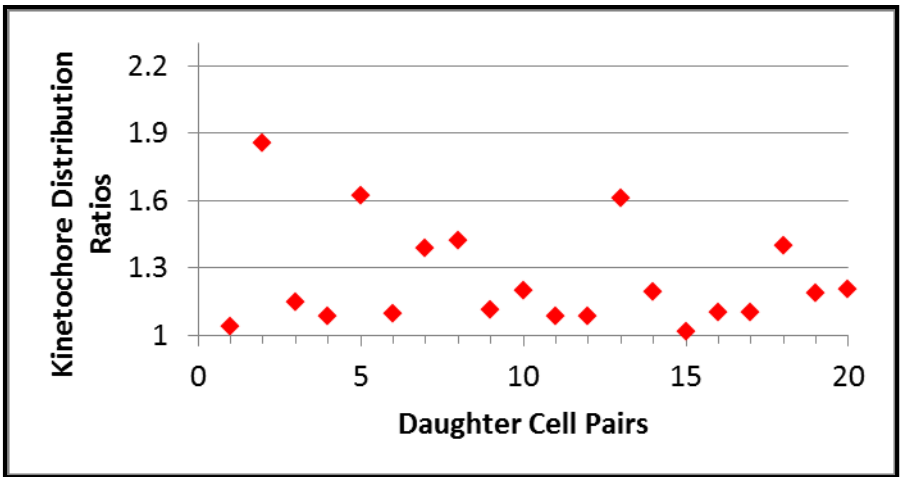

Figure 16 Kinetochore Distribution Ratios for Cells Treated with 50 nM Nocodazole

CHO cells were grown on coverslips in medium containing 2 mM hydroxyurea, 5 mM caffeine, and 50 nM nocodazole to produce nocodazole-treated MUG cells. Cells were then fixed in methanol, labeled with fluorescent antibodies, and mounted on slides with a medium containing DAPI®. A confocal microscope with a 1.4 NA / 100x plan apochromat lens was used to obtain a Z-stack. Microtubules (red), kinetochores (green), DNA (blue). ImageJ software was used to measure the total fluorescence intensity of kinetochore signal in each member of each daughter cell pair, and a kinetochore distribution ratio was calculated for each pair. For ratios less than 1, the inverse was taken so that all ratios used for analysis were greater than 1.

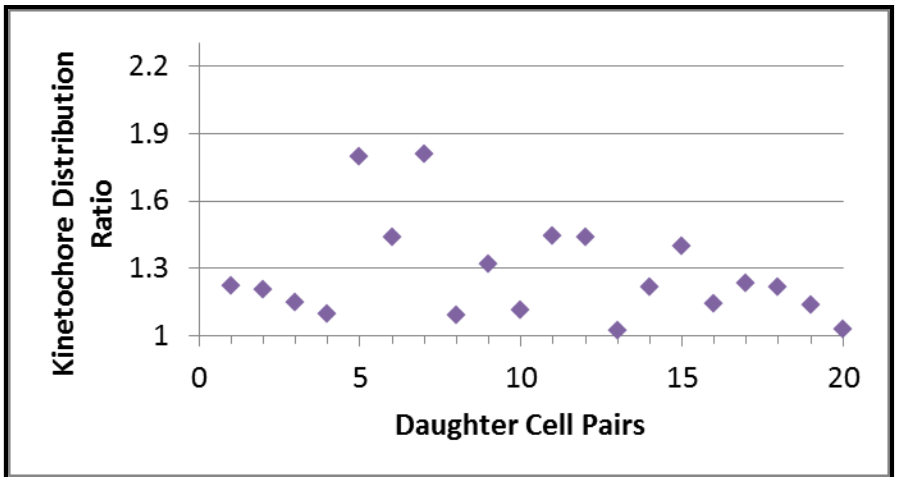

Figure 17 Kinetochore Distribution Ratios for 4C MUG Cells

CHO cells were grown on coverslips in medium containing 5 μM cytochalasin D before being treated with 2 mM hydroxyurea and 5 mM caffeine to produce 4C MUG cells. Cells were then fixed in methanol, labeled with fluorescent antibodies, and mounted on slides with a medium containing DAPI®. A confocal microscope with a 1.4 NA / 100x plan apochromat lens was used to obtain a Z-stack. Microtubules (red), kinetochores (green), DNA (blue). ImageJ software was used to measure the total fluorescence intensity of kinetochore signal in each member of each daughter cell pair, and a kinetochore distribution ratio was calculated for each pair. For ratios less than 1, the inverse was taken so that all ratios used for analysis were greater than 1.

CHAPTER V

DISCUSSION

The Effects of Low-Dose Taxol and Nocodazole on Lagging Kinetochores

One of the most unusual features of MUG cells is their ability to enter anaphase despite having numerous merotelic kinetochore-microtubule attachments in early mitosis. The results of this study show that in an unperturbed population, the percentage of MUG cells displaying lagging kinetochores (15%) is approximately the same as that of control cells (10%). This would suggest that MUG cells minimize merotelic attachments as efficiently as untreated CHO cells do. Although the lagging observed in MUGs and untreated CHO cells was similar in frequency, in one case, the lagging in MUGs was dramatically different *qualitatively*, with far more ACA signal in the midbody than in any of the controls (Figure 18). At first glance, this seems to suggest that MUGs might be more susceptible to lagging in ways that are not immediately apparent. However, another explanation is simpler: this DCP is very large relative to other MUG DCPs, and is comparable in size to a 4C MUG cell. As discussed below, it was not uncommon to see a lot of kinetochore signal in the midbody of those cells. Therefore, this cell might simply be a spontaneously-generated 4C MUG.

In cultured cells, microtubule-perturbing drugs are associated with an increased frequency of lagging chromosomes (Salmon et al., 2005). In this study, we found that the use of either taxol (5 nM) or nocodazole (25 nM or 50 nM) leads to dramatically

increased frequencies of lagging kinetochores in MUG cells. No effect on lagging was observed with 1 nM taxol, which is presumably too low a concentration to cause the effect seen at 5 nM. One interpretation of these data is that normal microtubule dynamics are required to prevent lagging in MUG cells.

Presumably, MUG cells recognize and reduce merotelic attachments before anaphase through an Aurora B kinase mechanism. Aurora B is known to mediate error correction in cultured cells (Hauf et al., 2003; Tanaka et al., 2002), although the SAC is not activated by merotely (Musacchio and Salmon, 2007). The pattern of lagging we report with microtubule perturbation could be caused in two ways: 1) the drugs could prevent the cell from reducing the number of merotelic attachments; or 2) they could re-introduce merotely that had already been corrected.

The experiments described here are insufficient to determine which of these proposals is correct. However, either mechanism requires that MUG cells distinguish merotelic attachments from monotelic ones (in which a kinetochore is linked to only one spindle pole), which is the only arrangement that should allow MUG kinetochores to be distributed to different DCs (Figure 19). Some researchers have suggested that unstable kinetochore-microtubule attachments delay anaphase and allow the cell to correct them, and that only when all of the cell's kinetochore-microtubule attachments are *stable* is anaphase initiated (Morgan, 2007). An obvious question follows from this proposal: What are the differences between merotelic and monotelic attachments that cause the former to be unstable but the latter stable?

One possibility is that merotelic kinetochore-microtubule attachments in MUGs, unlike merotelic attachments in untreated cells, might abnormally distort the kinetochore.

Figure 19 summarizes possible kinetochore orientations in both MUGs and control cells. A requirement that stable kinetochore-microtubule attachments be end-on attachments that are perpendicular to the plane of the kinetochore, for example, could explain why balanced merotely (leading to lagging kinetochores) is rarely found in MUG cells. According to this model, the unstable interactions in the merotelically-attached kinetochore would be reduced, leaving only monotelic, stable ones. In fact, in electron micrographs of control cells, microtubules are always perpendicular to the plane of the flat kinetochore surface.

Here it is important to distinguish between merotelic attachments in MUG cells and controls. Merotely in unperturbed cells can be balanced or unbalanced. In both cases, the normal amphitelic attachments (with each of the paired kinetochores attached to opposite poles) would be supplemented by additional attachments to the pole opposite that kinetochore. If there were fewer additional attachments to the distal than to the proximal pole, then merotely would be unbalanced. However, if the kinetochore had a similar number of attachments to both its proximal and distal poles, then its merotely would be balanced.

As demonstrated in the diagram in Figure 19, merotely in MUGs has different implications for kinetochore-microtubule arrangement and stability. Two features of the MUG kinetochore underlie these differences: first, in electron micrographs, the MUG kinetochore is seen as curved, not flat; and second, the kinetochore's orientation with respect to the spindle pole is not spatially constrained by pairing with a sister. In this case, balanced merotelic attachments would not be perpendicular to the plane of the kinetochore, and would therefore be unstable. The only stable attachments would be

monotelic (attachments to a single pole). A limited central region of the kinetochore would be able to make attachments that were both perpendicular to the kinetochore plate and emanating from the spindle pole. In the model presented here, only those attachments would be recognized by the cell as stable and satisfy the SAC. Others would be eliminated by the cell's error correction system.

The Effect of Increased Kinetochore Number on Lagging Kinetochores

MUG cells with a 4C kinetochore number were more likely than cells with a 2C kinetochore number to have lagging kinetochores. Because 4C is the typical complement of kinetochores found in diploid cells during mitosis, it is interesting that 4C MUG cells are more likely than 2C MUGs or control cells to have lagging kinetochores. One explanation that is consistent with this model of attachment stability is that the merotely found in 4C MUG cells, which is far greater than in typical cells, is simply more than they can correct. In one study, lagging chromosomes were observed in only 1% of untreated PtK1 cells. Kinetochore-microtubule attachments were analyzed in 11 cells with lagging chromosomes: nine cells had merotelic attachments, and two were detached from the mitotic spindle (Cimini et al., 2001).

Another puzzling question arises: If merotelic attachments are unstable, why are lagging kinetochores observed in MUG cells? That is, how does a subset of MUG cells (those having the 4C kinetochore number or those treated with taxol or nocodazole), with their merotelic attachments arranged to favor lagging kinetochores, enter anaphase at all? The answers offered in merotely studies of unperturbed cells are not particularly enlightening here (Cimini et al., 2004; Cimini et al., 2002; Cimini et al., 2001; Cimini et al., 2003), since the merotelically-attached MUG kinetochore can assume various

orientations with respect to the spindle pole, while the typical kinetochore (when paired and aligned at the metaphase plate) must face the pole. Low doses of taxol have been reported to stabilize attachments in cells, such that the duration of mitosis is shortened and cell division proceeds without the correction of unorthodox attachments (Yang et al., 2009). However, this argument is not very satisfactory to explain the lagging rate of the nocodazole-treated and 4C groups, since nocodazole and taxol have opposite effects on microtubules, and kinetochore number should have no effect (recall that the cytochalasin D that was used to create the 4C condition was washed out before the MUG procedure was begun).

Perhaps the most parsimonious explanation that can be plausibly advanced is the existence of a mechanism that overrides the SAC in the setting of excessive or long-standing attachment errors. In the taxol and nocodazole treatment conditions, it is possible that the presence of the drug contributes to premature entry into anaphase. In fact, taxol has been reported to shorten the duration of mitosis by stabilizing unorthodox attachments (Yang et al., 2009). However, it is implausible that treatment with nocodazole, which is known to lead to kinetochore-microtubule *detachment*, would produce the same outcome, making this argument hard to support. Finally, the possibility that some of the kinetochore-microtubule attachments that produce lagging kinetochores in MUGs are not merotelic cannot be discounted, although this hypothesis is hard to imagine in light of the model presented above.

The Effects of Taxol, Nocodazole, and Kinetochore Number on Kinetochore Distribution Ratios

Although the distribution of kinetochores to DCPs in MUGs may be conceived of as a stochastic process, here we report preliminary evidence that spindle-perturbing drugs can affect this distribution. On average, the KDR of the NOC-50 and TAX-5 groups is not significantly different from that of the CHO group, and these drug treatment groups have fewer individual DCPs with KDRs outside the range of controls than do the MUG cells treated with lower concentrations of microtubule-perturbing drugs. How treatment with these drugs could *improve* the KDR of MUG cells, such that they behave more like controls, is not obvious. In fact, if MUG cells always entered anaphase with monotelic attachments, it is hard to see how this KDR could be improved by any means. Therefore, these data suggest that at least a portion of kinetochore-microtubule attachments in MUG cells (even when untreated with additional drugs) have some other orientation that satisfies the cell's attachment stability requirements. Increasing the kinetochore number did not affect the KDR in MUG cells.

Kinetochore-microtubule attachment, anaphase initiation, and kinetochore distribution are complex cellular processes, and a complete model of mitosis should account for the behavior of both unperturbed cells and MUGs. Specifically, MUG cells do not require centromeric (interkinetochore) tension to satisfy the SAC; they appear to have a robust merotely correction mechanism; and merotely correction seems to be sensitive to microtubule turnover. A model of kinetochore-microtubule attachment in which microtubules bound perpendicular to the kinetochore plate are stabilized, while other orientations are destabilized and corrected, is consistent with these data and electron microscopy images from unperturbed cells. Although these descriptive studies

cannot test this model fully, this work should provide useful information for mechanistic studies in the future.

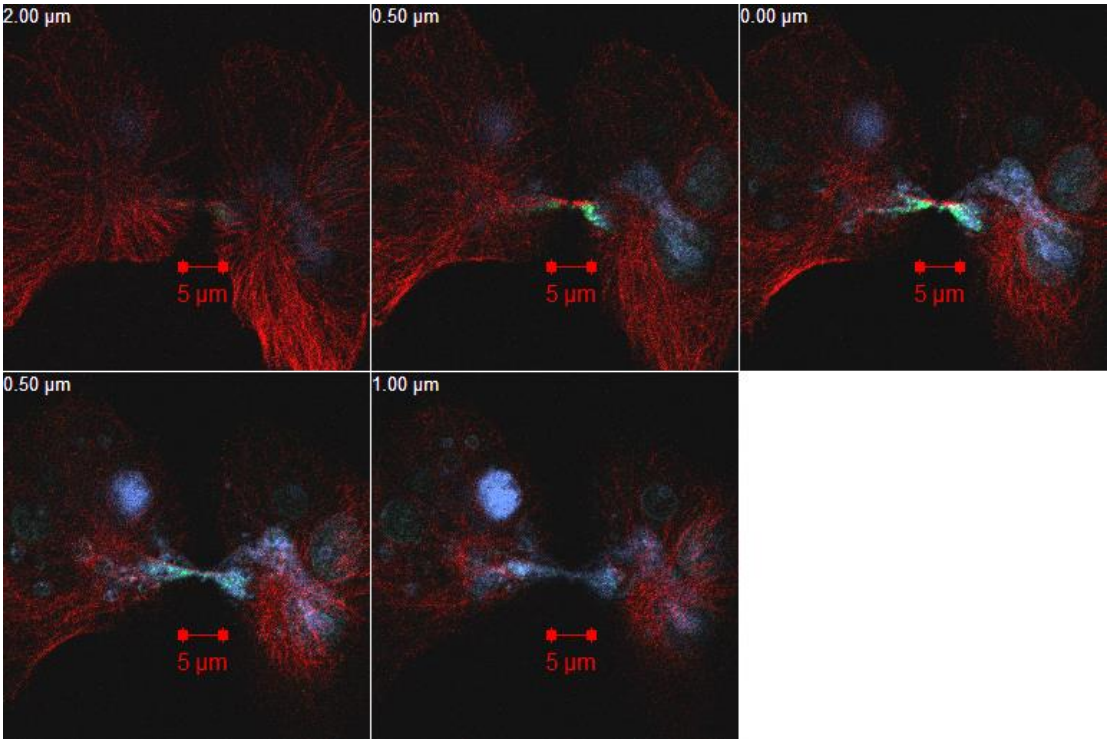

Figure 18 A Z-Stack of a MUG Cell with a Large Number of Lagging Kinetochores

CHO cells were grown on coverslips with in medium containing 2 mM hydroxyurea and 5 mM caffeine to produce MUG cells. Cells were fixed on coverslips in methanol, labeled with fluorescent antibodies, and mounted on slides with a medium containing DAPI®. A confocal microscope with a 1.4 NA / 100x plan apochromat lens was used to obtain a Z-stack. Microtubules (red), kinetochores (green), DNA (blue). Lagging kinetochores are visible in slices two through four.

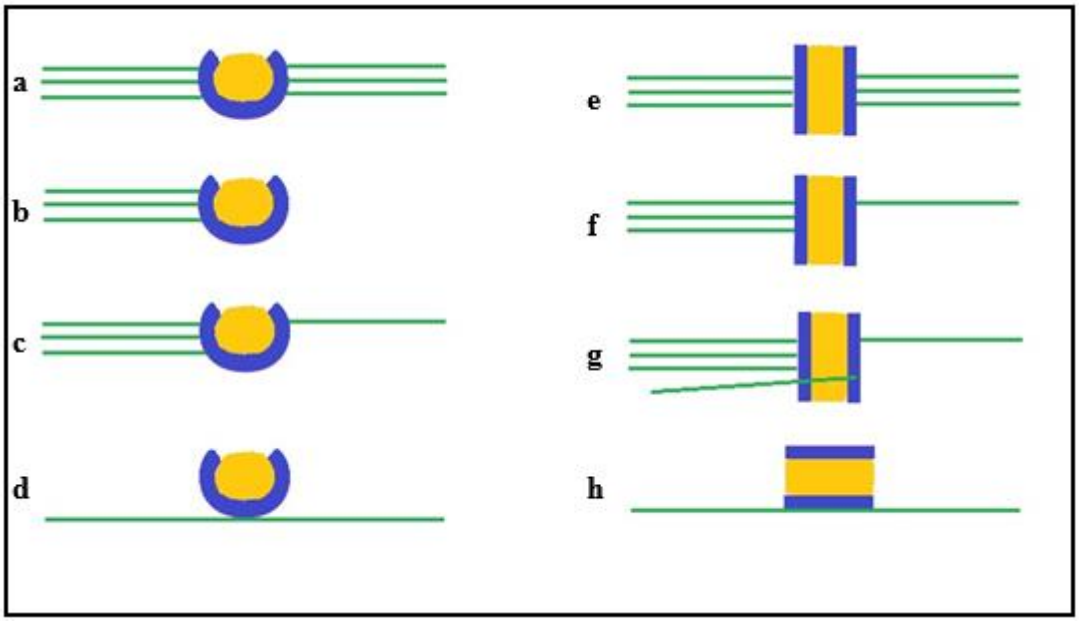

Figure 19 Possible Microtubule-Kinetochore Interactions in MUG and CHO Cells

Left: MUG cells can have a) balanced merotelic, b) monotelic, c) unbalanced merotelic, or d) lateral attachments. Microtubules (green), kinetochores (blue), chromatin (yellow).

Right: CHO cells can have e) balanced amphitelic, f) unbalanced amphitelic, g) merotelic, or h) lateral attachments. Microtubules (green), kinetochores (blue), chromatin (yellow).

REFERENCES

Ahonen, L.J., M.J. Kallio, J.R. Daum, M. Bolton, I.A. Manke, M.B. Yaffe, P.T. Stukenberg, and G.J. Gorbsky. 2005. Polo-like kinase 1 creates the tension-sensing 3F3/2 phosphoepitope and modulates the association of spindle-checkpoint proteins at kinetochores. *Current Biology*. 15:1078-1089.

Bergen, L., R. Kuriyama, and G. Borisy. 1980. Polarity of microtubules nucleated by centrosomes and chromosomes of Chinese hamster ovary cells in vitro. *Journal of Cell Biology*. 84:151-159.

Biggins, S. 2013. The composition, functions, and regulation of the budding yeast kinetochore. *Genetics*. 194:817-846.

Brenner, S., D. Pepper, M.W. Berns, E. Tan, and B.R. Brinkley. 1981. Kinetochore structure, duplication, and distribution in mammalian cells: analysis by human autoantibodies from scleroderma patients. *Journal of Cell Biology*. 91:95-102.

Brinkley, B.R., and E. Stubblefield. 1966. The fine structure of the kinetochore of a mammalian cell in vitro. *Chromosoma*. 19:28-43.

Brinkley, B.R., R.P. Zinkowski, W.L. Mollon, F.M. Davis, M.A. Pisegna, M. Pershouse, and P.N. Rao. 1988. Movement and segregation of kinetochores experimentally detached from mammalian chromosomes. *Nature*. 336:251-254.

Cheeseman, I.M., J.S. Chappie, E.M. Wilson-Kubalek, and A. Desai. 2006. The conserved KMN network constitutes the core microtubule-binding site of the kinetochore. *Cell*. 127:983-997.

Cheeseman, I.M., and A. Desai. 2008. Molecular architecture of the kinetochore-microtubule interface. *Nature Reviews: Molecular Cell Biology*. 9:33-46.

Cheeseman, I.M., S. Niessen, S. Anderson, F. Hyndman, J.R. Yates, 3rd, K. Oegema, and A. Desai. 2004. A conserved protein network controls assembly of the outer kinetochore and its ability to sustain tension. *Genes & Development*. 18:2255-2268.

Chen, J.-G., and S.B. Horwitz. 2002. Differential mitotic responses to microtubule-stabilizing and -destabilizing drugs. *Cancer Research*. 62:1935-1938.

Cimini, D. 2007. Detection and correction of merotelic kinetochore orientation by Aurora B and its partners. *Cell Cycle*. 6:1558-1564.

Cimini, D., L.A. Cameron, and E.D. Salmon. 2004. Anaphase spindle mechanics prevent mis-segregation of merotelically oriented chromosomes. *Current Biology*. 14:2149-2155.

Cimini, D., D. Fioravanti, E.D. Salmon, and F. Degrassi. 2002. Merotelic kinetochore orientation versus chromosome mono-orientation in the origin of lagging chromosomes in human primary cells. *Journal of Cell Science*. 115:507-515.

Cimini, D., B. Howell, P. Maddox, A. Khodjakov, F. Degrassi, and E.D. Salmon. 2001. Merotelic kinetochore orientation is a major mechanism of aneuploidy in mitotic mammalian tissue cells. *Journal of Cell Biology*. 153:517-527.

Cimini, D., B. Moree, J.C. Canman, and E.D. Salmon. 2003. Merotelic kinetochore orientation occurs frequently during early mitosis in mammalian tissue cells and error correction is achieved by two different mechanisms. *Journal of Cell Science*. 116:4213-4225.

Deeley, E.M., B.M. Richards, P.M. Walker, and H.G. Davies. 1954. Measurements of Feulgen stain during the cell-cycle with a new photo-electric scanning device. *Experimental Cell Research*. 6:569-572.

DeLuca, J.G., W.E. Gall, C. Ciferri, D. Cimini, A. Musacchio, and E.D. Salmon. 2006. Kinetochore microtubule dynamics and attachment stability are regulated by Hec1. *Cell*. 127:969-982.

Evans, E.B. 2009. CHO-human hybrid cells as models for human chromosome non-disjunction. Mississippi State University, Mississippi State.

Flemming, W. 1882. Zellsubstanz, Kern und Zelltheilung. Vogel, Leipzig.

Foley, E.A., and T.M. Kapoor. 2013. Microtubule attachment and spindle assembly checkpoint signalling at the kinetochore. *Nature Reviews: Molecular Cell Biology*. 14:25-37.

Hartwell, L.H., J. Culotti, J.R. Pringle, and B.J. Reid. 1974. Genetic control of the cell division cycle in yeast. *Science*. 183:46-51.

Hartwell, L.H., J. Culotti, and B. Reid. 1970. Genetic control of the cell-division cycle in yeast. I. Detection of mutants. *Proceedings of the National Academy of Sciences*. 66:352-359.

Hauf, S., R.W. Cole, S. LaTerra, C. Zimmer, G. Schnapp, R. Walter, A. Heckel, J. van Meel, C.L. Rieder, and J.M. Peters. 2003. The small molecule Hesperadin reveals a role for Aurora B in correcting kinetochore-microtubule attachment and in maintaining the spindle assembly checkpoint. *Journal of Cell Biology*. 161:281-294.

Hsu, T.C., W.C. Dewey, R.M. Humphrey, and V. Monesi. 1962. Radiosensitivity of cells of Chinese hamster in vitro in relation to the cell cycle. *Experimental Cell Research*. 27:441-452.

Inoué, S., and H. Sato. 1967. Cell motility by labile association of molecules: The nature of mitotic spindle fibers and their role in chromosome movement. *Journal of General Physiology*. 50:259-292.

Jackson, S.P. 1996. DNA damage detection by DNA dependent protein kinase and related enzymes. *Cancer Surveys*. 28:261-279.

Johnson, M.K., and D.A. Wise. 2010. Distribution of kinetochore fragments during mitosis with unreplicated genomes. *Cytoskeleton (Hoboken, N.J.)*. 67:172-177.

Johnson, R.T., and P.N. Rao. 1970. Mammalian cell fusion: induction of premature chromosome condensation in interphase nuclei. *Nature*. 226:717-722.

Jokelainen, P.T. 1967. The ultrastructure and spatial organization of the metaphase kinetochore in mitotic rat cells. *Journal of Ultrastructure Research*. 19:19-44.

Jordan, M.A., D. Thrower, and L. Wilson. 1992. Effects of vinblastine, podophyllotoxin and nocodazole on mitotic spindles: Implications for the role of microtubule dynamics in mitosis. *Journal of Cell Science*. 102 (Pt 3):401-416.

Kiefer, B., H. Sakai, A.J. Solari, and D. Mazia. 1966. The molecular unit of the microtubules of the mitotic apparatus. *Journal of Molecular Biology*. 20:75-79.

Knowlton, A.L., W. Lan, and P.T. Stukenberg. 2006. Aurora B is enriched at merotelic attachment sites, where it regulates MCAK. *Current Biology*. 16:1705-1710.

Koç, A., L.J. Wheeler, C.K. Mathews, and G.F. Merrill. 2004. Hydroxyurea arrests DNA replication by a mechanism that preserves basal dNTP pools. *Journal of Biological Chemistry*. 279:223-230.

Leland, H.H., and T.A. Weinert. 1989. Checkpoints: Controls that ensure the order of cell cycle events. *Science*. 246:629-634.

Liu, D., and M.A. Lampson. 2009. Regulation of kinetochore-microtubule attachments by Aurora B kinase. *Biochemical Society Transactions*. 37:976-980.

Maresca, T.J., and E.D. Salmon. 2009. Intrakinetochore stretch is associated with changes in kinetochore phosphorylation and spindle assembly checkpoint activity. *Journal of Cell Biology*. 184:373-381.

Martin, D., Jr., G.M. Tomkins, and D. Granner. 1969. Synthesis and induction of tyrosine aminotransferase in synchronized hepatoma cells in culture. *Proceedings of the National Academy of Sciences*. 62:248-255.

Masui, Y., and C.L. Markert. 1971. Cytoplasmic control of nuclear behavior during meiotic maturation of frog oocytes. *Journal of Experimental Zoology*. 177:129-145.

Matsuoka, S., M. Huang, and S.J. Elledge. 1998. Linkage of ATM to cell cycle regulation by the Chk2 protein kinase. *Science*. 282:1893-1897.

McIntosh, J.R., E. O'Toole, K. Zhudenkov, M. Morphew, C. Schwartz, F.I. Ataullakhanov, and E.L. Grishchuk. 2013. Conserved and divergent features of kinetochores and spindle microtubule ends from five species. *Journal of Cell Biology*. 200:459-474.

Monesi, V. 1962. Relation between x-ray sensitivity and stages of the cell cycle in spermatogonia of the mouse. *Radiation Research*. 17:809-838.

Morgan, D.O. 1997. Cyclin-dependent kinases: Engines, clocks, and microprocessors. *Annual Review of Cell and Developmental Biology*. 13:261-291.

Morgan, D.O. 2007. The Cell Cycle: Principles of Control. New Science Press ; Sinauer Associates, London; Sunderland, MA.

Musacchio, A., and E.D. Salmon. 2007. The spindle-assembly checkpoint in space and time. *Nature Reviews: Molecular Cell Biology*. 8:379-393.

O'Connell, C.B., J. Loncarek, P. Hergert, A. Kourtidis, D.S. Conklin, and A. Khodjakov. 2008. The spindle assembly checkpoint is satisfied in the absence of interkinetochore tension during mitosis with unreplicated genomes. *Journal of Cell Biology*. 183:29-36.

Pinsky, B.A., and S. Biggins. 2005. The spindle checkpoint: Tension versus attachment. *Trends in Cell Biology*. 15:486-493.

Rao, P.N., and R.T. Johnson. 1970. Mammalian cell fusion: studies on the regulation of DNA synthesis and mitosis. *Nature*. 225:159-164.

Rasband, W.S. 1997-2014. ImageJ. U. S. National Institutes of Health, Bethesda, Maryland, USA.

Rieder, C.L. 1999. Mitosis and Meiosis / edited by Conly L. Rieder. *In* Methods in Cell Biology; v. 61. San Diego: Academic Press, 1999.

Rieder, C.L., and S.P. Alexander. 1990. Kinetochores are transported poleward along a single astral microtubule during chromosome attachment to the spindle in newt lung cells. *Journal of Cell Biology*. 110:81-95.

Salmon, E.D., D. Cimini, L.A. Cameron, and J.G. DeLuca. 2005. Merotelic kinetochores in mammalian tissue cells. *Philosophical Transactions of the Royal Society: Biological Sciences*. 360:553-568.

Sarkaria, J.N., E.C. Busby, R.S. Tibbetts, P. Roos, Y. Taya, L.M. Karnitz, and R.T. Abraham. 1999. Inhibition of ATM and ATR kinase activities by the radiosensitizing agent, caffeine. *Cancer Research*. 59:4375-4382.

Schlegel, R., and A.B. Pardee. 1986. Caffeine-induced uncoupling of mitosis from the completion of DNA replication in mammalian cells. *Science*. 232:1264-1266.

Sisken, J.E., and R. Kinosita. 1961. Timing of DNA synthesis in the mitotic cycle *in vitro*. *The Journal of Biophysical and Biochemical Cytology*. 9:509-518.

Swann, M.M. 1962. Gene replication, ultra-violet sensitivity and the cell cycle. *Nature*. 193:1222-1227.

Tanaka, T.U., N. Rachidi, C. Janke, G. Pereira, M. Galova, E. Schiebel, M.J. Stark, and K. Nasmyth. 2002. Evidence that the Ipl1-Sli15 (Aurora kinase-INCENP) complex promotes chromosome bi-orientation by altering kinetochore-spindle pole connections. *Cell*. 108:317-329.

Tanaka, T.U., M.J. Stark, and K. Tanaka. 2005. Kinetochore capture and bi-orientation on the mitotic spindle. *Nature Reviews: Molecular Cell Biology*. 6:929-942.

Uchida, K.S.K., K. Takagaki, K. Kumada, Y. Hirayama, T. Noda, and T. Hirota. 2009. Kinetochore stretching inactivates the spindle assembly checkpoint. *Journal of Cell Biology*. 184:383-390.

Van't Hof, J. 1968. Control of cell progression through the mitotic cycle by carbohydrate provision: I. Regulation of cell division in excised plant tissue. *Journal of Cell Biology*. 37:773-780.

Varma, D., and E.D. Salmon. 2012. The KMN protein network – chief conductors of the kinetochore orchestra. *Journal of Cell Science*. 125:5927-5936.

Waters, J.C., R.-H. Chen, A.W. Murray, and E.D. Salmon. 1998. Localization of Mad2 to kinetochores depends on microtubule attachment, not tension. *Journal of Cell Biology*. 141:1181-1191.

Wise, D.A., and B.R. Brinkley. 1997. Mitosis in cells with unreplicated genomes (MUGs): Spindle assembly and behavior of centromere fragments. *Cell Motility and the Cytoskeleton*. 36:291-302.

Xiao, H., P. Verdier-Pinard, N. Fernandez-Fuentes, B. Burd, R. Angeletti, A. Fiser, S.B. Horwitz, and G.A. Orr. 2006. Insights into the mechanism of microtubule stabilization by taxol. *Proceedings of the National Academy of Sciences*. 103:10166-10173.

Yang, Z., A.E. Kenny, D.A. Brito, and C.L. Rieder. 2009. Cells satisfy the mitotic checkpoint in Taxol, and do so faster in concentrations that stabilize syntelic attachments. *Journal of Cell Biology*. 186:675-684.

Zieve, G.W. 1984. Nocodazole and cytochalasin D induce tetraploidy in mammalian cells. *American Journal of Physiology - Cell Physiology*. 246:C154-156.